USGS
science for a changing world

Prepared in cooperation with the Wisconsin Department of Transportation

Flood-Frequency Characteristics of Wisconsin Streams

Scientific Investigations Report 2016–5140
Version 2.2, April 2020

U.S. Department of the Interior
U.S. Geological Survey

Cover. Aerial view of floodwaters of the White and Bad Rivers surrounding St. Mary Catholic Church, in Odanah, Wisconsin, during July 2016. Photo courtesy of the Bad River Band of the Lake Superior Chippewa Tribe.

Flood-Frequency Characteristics of Wisconsin Streams

By John F. Walker, Marie C. Peppler, Mari E. Danz, and Laura E. Hubbard

Prepared in cooperation with the Wisconsin Department of Transportation

Scientific Investigations Report 2016–5140
Version 2.2, April 2020

U.S. Department of the Interior
U.S. Geological Survey

U.S. Department of the Interior
RYAN K. ZINKE, Secretary

U.S. Geological Survey
William H. Werkheiser, Deputy Director
exercising the authority of the Director

U.S. Geological Survey, Reston, Virginia: 2017
First release: 2017
Revised: August 2017 (ver. 2.0)
Revised: December 2017 (ver. 2.1)
Revised: April 2020 (ver. 2.2)

For more information on the USGS—the Federal source for science about the Earth, its natural and living resources, natural hazards, and the environment—visit http://www.usgs.gov or call 1–888–ASK–USGS.

For an overview of USGS information products, including maps, imagery, and publications, visit http://store.usgs.gov/.

Suggested citation:
Walker, J.F., Peppler, M.C., Danz, M.E., and Hubbard, L.E., 2017, Flood-frequency characteristics of Wisconsin streams (ver. 2.2, April 2020): Reston, Virginia, U.S. Geological Survey Scientific Investigations Report 2016–5140, 33 p., 1 plate, 2 appendixes, https://doi.org/10.3133/sir20165140.

ISSN 2328-0328 (online)

Contents

Plate

[Available for download from https://doi.org/10.3133/sir20165140]

Figures

Tables

Conversion Factors

U.S. customary units to International System of Units

Multiply	By	To obtain
	Length	
inch (in.)	2.54	centimeter (cm)
inch (in.)	25.4	millimeter (mm)
foot (ft)	0.3048	meter (m)
mile (mi)	1.609	kilometer (km)
	Area	
acre	4,047	square meter (m^2)
square mile (mi^2)	2.590	square kilometer (km^2)
	Volume	
cubic mile (mi^3)	4.168	cubic kilometer (km^3)
acre-foot (acre-ft)	1,233	cubic meter (m^3)
	Flow rate	
cubic foot per second (ft^3/s)	0.02832	cubic meter per second (m^3/s)
cubic foot per second per square mile [$(ft^3/s)/mi^2$]	0.01093	cubic meter per second per square kilometer [$(m^3/s)/km^2$]
inch per hour (in/h)	0.0254	meter per hour (m/h)
	Hydraulic gradient	
foot per mile (ft/mi)	0.1894	meter per kilometer (m/km)

International System of Units to U.S. customary units

Multiply	By	To obtain
	Length	
meter (m)	3.281	foot (ft)
meter (m)	1.094	yard (yd)

Datum

Vertical coordinate information is referenced to the North American Vertical Datum of 1988 (NAVD 88).

Horizontal coordinate information is referenced to the North American Datum of 1983 (NAD 83).

Altitude, as used in this report, refers to distance above the vertical datum.

Supplemental Information

Water year is the 12-month period October 1 through September 30, designated by the calendar year in which the water year ends.

Flood-Frequency Characteristics of Wisconsin Streams

By John F. Walker, Marie C. Peppler, Mari E. Danz, and Laura E. Hubbard

Abstract

Flood-frequency characteristics for 360 gaged sites on unregulated rural streams in Wisconsin are presented for percent annual exceedance probabilities ranging from 0.2 to 50 using a statewide skewness map developed for this report. Equations of the relations between flood-frequency and drainage-basin characteristics were developed by multiple-regression analyses. Flood-frequency characteristics for ungaged sites on unregulated, rural streams can be estimated by use of the equations presented in this report. The State was divided into eight areas of similar physiographic characteristics. The most significant basin characteristics are drainage area, soil saturated hydraulic conductivity, main-channel slope, and several land-use variables. The standard error of prediction for the equation for the 1-percent annual exceedance probability flood ranges from 56 to 70 percent for Wisconsin Streams; these values are larger than results presented in previous reports. The increase in the standard error of prediction is likely due to increased variability of the annual-peak discharges, resulting in increased variability in the magnitude of flood peaks at higher frequencies. For regulated streams, a graphical method for estimating flood-frequency characteristics was developed from the relations of discharge and drainage area for selected annual exceedance probabilities. Graphs for the major regulated streams in Wisconsin are presented in the report.

Introduction

Flood-frequency information is needed for the design of bridges, culverts, highways, flood-protection structures, and for effective flood-plain management. This report includes a description of flood-frequency characteristics of Wisconsin streams where streamflow data are available, equations for estimating flood-frequency characteristics at ungaged sites, and a discussion of the development of the equations.

The study was done in cooperation with the Wisconsin Department of Transportation. The report is the sixth within a long-term study of flood-frequency characteristics of Wisconsin streams. Previous reports on this subject were done by Ericson (1961); Conger (1971); Conger (1981); Krug and others (1992); and Walker and Krug (2003). Other reports that include methods for estimating flood-frequency characteristics of Wisconsin streams were done by Wiitala (1965) and Patterson and Gamble (1968). Additional data used in this report increase the confidence in estimating techniques and supersede the frequency analyses and resulting regression equations published in previous reports.

The regression equations presented in this report were developed based on records from streamflow-gaging stations with little or no effect from urbanization or regulation. As such the regressions only apply to rural sites, and should not be used to predict peak discharges and frequencies for basins with more than minimal urban land-use characteristics. In addition, the regression equations are only valid for streams without substantial regulation. A dam on a stream or river does not constitute regulation unless the dam is used to control the flow during a flood. For sites on major rivers with substantial regulation, alternative techniques are presented for estimating peak discharges and frequencies.

Data Collection Network

Flood-peak data were retrieved from the NWISWeb internet service (U.S. Geological Survey NWISweb, 2013); data used in this study were collected at 154 crest-stage-gaging stations and 206 continuous-record streamflow-gaging stations located throughout the State (plate 1). Only the peak stage of a flood is recorded at a crest-stage station. The recorded maximum stage for each water year is converted to discharge by a stage-discharge relation for each crest-stage gage. At continuous-record streamflow-gaging stations, a continuous record of stream stage is recorded. The recorded stages for the water year are converted to discharge by a stage-discharge relation, and the largest peak discharge is selected. In some cases where backwater conditions exist, the largest peak discharge does not necessarily correspond to the largest stage. Streamflow-gaging stations with at least 10 years of record located on rural streams were selected for inclusion in the study, resulting in the selection of 360 stations. Flood-peak data are available for

81 crest-gage stations and for 122 continuous-record streamflow-gaging stations operated during the 2010 water year and from 73 crest-stage-gaging stations and 84 continuous-record streamflow-gaging stations that have been discontinued. Of the continuous-record stations, 47 are on streams that are regulated. Sites were classified as regulated based on knowledge of the flow system and hydrologic judgment. The 154 crest-stage-gaging stations are operated as part of the flood-frequency project. Most of the crest-stage-gaging stations have been operated since the late 1950s or early 1960s. Several stations were started around 1970 in northeastern Wisconsin when an initial analysis of the data determined the need for more data in this area. These two types of stations will be collectively referred to as streamflow-gaging stations hereafter.

Flood-Frequency Analysis

Flood-frequency analyses define the relation of flood-peak magnitude to probability of exceedance or recurrence interval. In previous reports (Ericson, 1961; Conger, 1971; Conger, 1981; Krug and others, 1992; and Walker and Krug, 2003) flood estimates have been reported in terms of a T-year flood based on selected values of the recurrence interval, T. Because the T-year nomenclature implies a regularity of occurrence, the terminology associated with flood-frequency estimates has shifted away from the T-year recurrence interval flood to the p-percent annual exceedance probability (AEP) flood. The p-percent AEP flood has a p-percentage chance that the flood will be exceeded in any year. Recurrence interval is the reciprocal of p-percent AEP divided by 100, and is the average number of years between exceedances. For example, a flood having a 1-percent AEP has a recurrence interval of 100 years. Throughout the remaining sections of this report the p-percent AEP terminology will be used to describe peak-streamflow frequency estimates.

Flood-frequency analyses were done for all rural streamflow-gaging stations where the period of record equaled or exceeded 10 years. Guidelines in Bulletin 17B (Interagency Advisory Committee on Water Data, 1982) were used to fit logarithms of annual peak discharges to the Pearson Type III distribution. For streamflow-gaging stations on unregulated streams, the generalized skew from the map described in the next section was weighted with the station skew to give a weighted skew. Estimates of discharges at p-percent AEP ranging from 50 to 0.2 percent for each station are given in appendix tables 2–1 through 2–9.

Streamflow-gaging stations on the main stem of the Wisconsin River received special treatment. Krug and House (1980) modeled the system of reservoirs and reservoir operation to simulate the flood peaks on the Wisconsin River for water years 1915 through 1976. The p-percent AEP floods given for the Wisconsin River in this study (appendix table 2–10) include the simulated peaks (Krug and House, 1980; appendix B) and the observed peaks for water years 1977 through 2008. These p-percent AEP floods are considered the best estimates of the flood potential of the existing system of reservoirs and reservoir operating policies (appendix table 2–10).

Skewness Analysis

The map provided in Bulletin 17B (Interagency Advisory Committee on Water Data, 1982) provides a general depiction of skewness across the conterminous United States, and as such does not provide a lot of detail within an individual state. Further, the general map is based on skewness calculated with data collected through the 1973 water year, thus omits 37 years of current flooding information. Use of the general map in Bulletin 17B is recommended only in cases where a detailed skewness analysis has not been developed. Because the skewness values in the general map do not reflect current flooding conditions, a detailed analysis was carried out for Wisconsin.

Following the guidelines described in chapter V, section B–3 (Interagency Advisory Committee on Water Data, 1982), gages with at least 25 years of record through the 2008 water year were selected for analysis. Values of the station skewness as calculated by the PeakFQ software application (Flynn and others, 2006) were used. The technique used to develop an isoline map is based on the approach used to develop the skewness map in Minnesota (Lorenz, 1997). The procedure uses a locally weighted regression technique (Cleveland and Devlin, 1988) to relate the individual skewness values to location as determined by the latitude and longitude of each streamflow-gaging station. A second-order model was selected, and the proportion of data used at each site was varied from 40 to 95 percent in increments of 5 percent. For each proportion, the mean-squared error and bias of the model fit was calculated. The final model chosen was based on minimizing the bias for a reasonable amount of variability as measured by the mean-squared error, resulting in 55 percent proportion of data used in the fitting process. This results in a mean-squared error of 0.309. The mean-squared error of the general Bulletin 17B map is 0.302; however, the mean-squared error for the general map computed by using flood-peak records updated through 2008 is 0.344, thus the new isoline map is a considerable improvement over the general map. The resulting skewness map is depicted in figure 1.

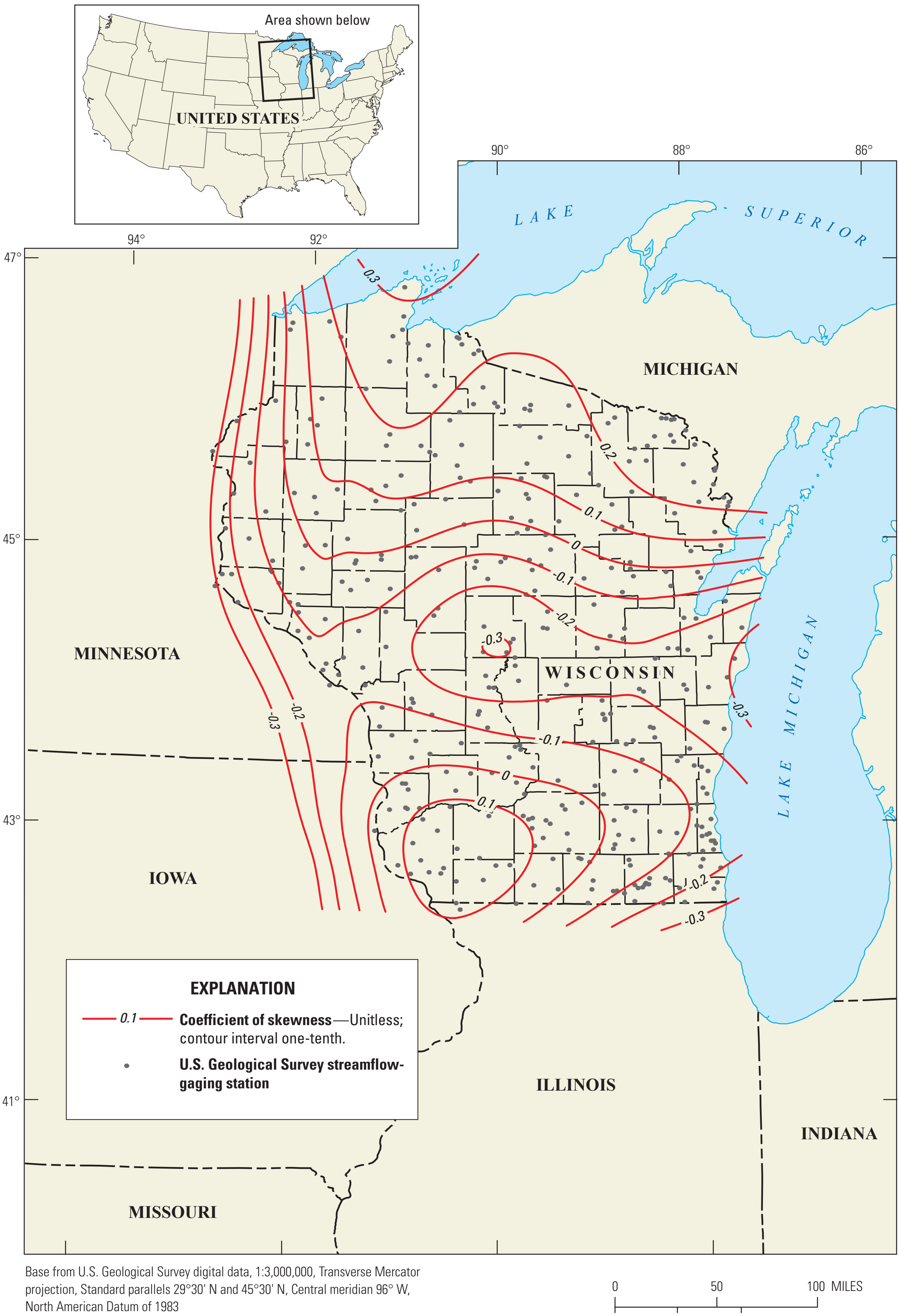

Figure 1. Distribution values for coefficient of skewness in Wisconsin.

Historical Flood Records

Historical research was used to determine if there was a flood of greater magnitude than the 2008 flood outside of the period of record. The date of a large flood outside of the official period of record that was not larger than the 2008 flood can be used to expand the length of the historical record. This allows us to assume that the 2008 flood is the peak of record for a longer period of time. When a high outlier peak flood is framed in a longer historical record, the estimate of the flood magnitude is more accurate due to a better fit of the log Pearson distribution to the peak of record. Nine streamflow-gaging stations with high outliers were chosen following the flood of June 2008 (Fitzpatrick and others, 2008) for additional historical research: Oak Creek at South Milwaukee, Wisconsin (Wis.); Root River at Racine, Wis.; West Branch Baraboo River at Hillsboro, Wis.; Baraboo River near Baraboo, Wis.; Kickapoo River at La Farge, Wis.; Kickapoo River at Steuben, Wis.; Beaverdam River at Beaver Dam, Wis.; Bark River near Rome, Wis.; and Yahara River at Windsor, Wis. (table 1). For these nine locations, the 2008 peaks were identified as high outliers using the high outlier criterion in Bulletin 17B (Interagency Advisory Committee on Water Data, 1982).

Table 1. Streamflow-gaging stations with historical research and extended periods of record.

[Wis., Wisconsin; CSG, crest-stage gage station; USGS, U.S. Geological Survey]

USGS station number	Station name	Drainage area, in square miles	Year site established	Instrumented period of record	Earliest historical flood year found	Additional years added to the record	Notes and citations
04087204	Oak Creek at South Milwaukee, Wis.	25.0	1964	45	1837	127	Historical CSG, no record in files collected from gage file; "Evergreen City Times, June 5, 1858."
04087240	Root River at Racine, Wis.	190	1964	45	1843	121	USGS historical note in Station Description file mentions a newspaper article on the 1843 flood. No copy of article found.
05404116	South Branch Baraboo River at Hillsboro, Wis.	39.1	1988	21	[1]1859	129	See station number 05405000.
05405000	Baraboo River near Baraboo, Wis.	609	1914	75	[1]1859	55	Freshet, ice dominated flood; "The Baraboo Republic, March 17, 1859."
05408000	Kickapoo River at La Farge, Wis.	266	1939	70	1881	58	USGS historical note on file; "The Racine Daily Journal, June 13, 1899."
05410490	Kickapoo River at Steuben, Wis.	687	1934	75	1881	53	See station number 05408000; USGS Water-Supply Paper 771.
05425912	Beaver Dam River at Beaver Dam, Wis.	157	1986	23	1921	65	Written commun., Ritchie Piltz, City Engineer, 2010.
05426250	Bark River near Rome, Wis.	122	1984	25	1959	25	"Wisconsin Rapids Daily Tribune, April 6, 1959."
05427718	Yahara River at Windsor, Wis.	73.6	1976	24	1924	52	"The Wisconsin State Journal, August 4, 1924."

[1] Ice dominated flood.

Historical research included database and general internet searches combined with local interviews and historical documents (both public and USGS files) to determine the effective period of record for each of the nine streamflow-gaging stations. Historical records from counties surrounding each of the locations also were examined for indications or previous floods that were not recorded locally. No surveying or additional fieldwork was completed to ensure that the historical floods were indeed lower than the 2008 peak. No historical information was detailed enough (nor were photographs found) that would have allowed for such determinations.

Library searches and literature reviews at the state, county, and local levels were used to acquire historical documents such as newspaper articles and photographs on major floods. BadgerLink, a database provided through the Wisconsin State Historical Society, and Access Newspaper ARCHIVE were two databases used for locating newspaper articles. Web sites for counties, such as Milwaukee, Sauk, and Dodge, were used to locate potential interviewees and search local historical collections. Wisconsinheritage.org offered brief information on major floods around the state. For example, "Wolf River, 1880: The same storms raised streams and creeks in northeastern Wisconsin, and bridges at Keshena, Belle Plaine and Shiocton were all swept away as those communities were inundated" (wisconsinheritage.org, accessed June 2012). The Wisconsin State Historical Society database, MadCat, allowed access to the University of Wisconsin-Madison's library system and the Society's collections. Valuable information on major floods came from the county history books at the Society. Internal USGS files containing notes, collection data, and gage peaks at each of the nine sites were reviewed to ensure that all historical notes and anecdotes were recorded for the nine sites.

Interviews were conducted by way of the county historical societies and suggestions given by those contacts. The U.S. Army Corps of Engineers, the Sauk County Historical Society, the Beaver Dam City Engineer's office, and the Highway Department were contacted.

The historical flood research resulted in adding from 25 to 129 years to the period of record for the streamflow-gaging stations (table 1). For each location, a year was chosen based on the soundness of the historical research. In some cases, notes were found about older floods, but it was not clear that the flood was at the community or site of interest but perhaps only in the surrounding area. When these extended periods of record are combined with a recent large flood (such as June 2008) the estimated discharges for floods with higher frequencies are greatly improved as a result of reduced residuals for higher frequency floods (Eash and Koppensteiner, 1997).

Regression Analysis and Flood-Frequency Equations

Multiple-regression analysis was used to estimate the relation between flood discharges for p-percent annual exceedance probability (AEP) floods and drainage-basin characteristics for 143 selected continuous-record streamflow-gaging stations and 141 crest-stage-gaging stations in Wisconsin. The multiple-regression technique is a means of transferring flood-peak characteristics from sites where observed data are available to ungaged locations. The relation is presented by flood-frequency equations.

The regression equations are used to relate the most significant drainage-basin characteristics (independent variables) to flood-peak characteristics (dependent variables; Q_{50p}, Q_{20p}..., $Q_{0.2p}$). The multiple-regression model can be expressed in the following form:

$$Q_{xp} = C_0 X_1^{\beta_1} X_2^{\beta_2} \text{ - - - } X_m^{\beta_m} \tag{1}$$

where

Q_{xp} is flood magnitude, in cubic feet per second, having an x-percent annual exceedance;

C_0 is a regression constant defined by regression analysis;

$X_1, X_2 ..., X_m$ are basin characteristics; and

$\beta_1, \beta_2, \ldots, \beta_m$ are regression coefficients defined by regression analysis.

This form of the multiple-regression model is achieved by applying a linear regression to the logarithms of the dependent and independent variables.

The principal method of regression analysis used in the study is called generalized least squares (GLS) and was developed by Tasker and others (1986) and Stedinger and Tasker (1985). This method was used because of its theoretical advantages over the ordinary least squares (OLS) method and the conventional weighted least squares (WLS) method.

In the OLS method, all the estimates of p-percent AEP floods for a particular value of p are implicitly assumed to have equal variance; that is, the flood estimate at each streamflow-gaging station is assumed to be as accurate as the flood estimates at all other streamflow-gaging stations used in the regression, regardless of record length and at-site variability. Furthermore, in the OLS method, the concurrent flood peaks at different sites are assumed to be uncorrelated or independently distributed. In general, these two conditions are not met by flood-peak records. The accuracy of the p-percent AEP flood varies with the length of record and at-site variability. Many concurrent annual floods in an area are correlated because the streamflow-gaging stations in the area are often subject to similar weather systems.

In the GLS method, the variable accuracy of the p-percent AEP floods and the correlation between streamflow-gaging stations are included in the analysis. In addition, information is provided for analyzing the network of streamflow-gaging stations. This network analysis capability can be used to design future studies by indicating potential locations for new gages.

Independent Variables

A diverse set of basin characteristics and climatic variables was determined for each streamflow-gaging station selected for analysis as potential explanatory variables to be used in the regression analysis. The complete set of basin characteristics used in the regression analysis is listed for each streamflow-gaging station in appendix 2 (table 2–11). The selected independent variables are defined as follows:

Drainage Area (A), in square miles, is the area contributing directly to surface runoff.
Determined by calculating the geometry of a basin polygon coverage within a Geographic Information System (GIS) coverage. The basin polygon coverage is associated with the NHDPlus Version 2 datasets, including the Watershed Boundary Dataset (U.S. Geological Survey and others, 2012). ArcHydro, a suite of GIS tools for analyzing hydrologic geospatial data, was used to delineate basins for each of the streamgage locations in the Wisconsin network. The drainage areas determined with the automated technique were compared to those determined by using manual techniques from a previous version of this report (Walker and Krug, 2003). The median difference between the two techniques was less than 0.1 percent, and nearly 90 percent of the sites had differences within 5 percent. The percent differences exceeding 5 percent were due to either (1) small values of drainage area resulting in exaggerated percent differences, or (2) adjustments to drainage area used in the previous report to account for noncontributing areas.

Main-channel slope (S), in feet per mile, is the slope of the main channel between the 10th and 85th percentile of the distance between the gaging station and the basin boundary.
Main-channel slope was determined with the ArcHydro tool by identifying the main channel based on the 30-meter (m) resolution digital elevation models, locating the 10- and 85-percentile distance points, and extracting the altitude of the two points. The difference in altitude between the points was divided by the main channel stream length between the points to compute the slope in feet per mile.

Saturated hydraulic conductivity (Ksat), in micrometers per second, is the ease with which water can move through a medium (appendix fig. 2–1).
Determined by (1) extracting K_{sat} data from SSURGO datasets for each county using U.S. Department of Agriculture Soil Data Viewer software (http://soils.usda.gov/sdv/) with the following rating options: Aggregation method = weighted average, Tie Break Rule = fastest, Layer Options = surface layer, (2) compiling the data into a statewide map, (3) creating a raster grid from the statewide data using a cell size of 30 m, and (4) calculating the mean of each basin with the Zonal Statistics geoprocessing tool within Spatial Analyst in ArcGIS 10.1.

Snow, 1971–2000 mean annual snowfall in each basin (DVD from www.climatesource.com).
Determined by (1) interpolating point snowfall data to a raster grid using ordinary kriging with linear semivariogram (tool contained within ArcGIS 10.1), and (2) calculating the mean of each basin using zonal statistics (appendix fig. 2–2).

Precipitation, 1971–2000 mean annual precipitation in the basin (DVD from www.climatesource.com).
Determined by (1) interpolating point precipitation data to a raster grid using ordinary kriging with linear semivariogram (tool contained within ArcGIS 10.1), and (2) calculating the mean of each basin using zonal statistics (appendix fig. 2–3).

24-hour precipitation indices, (2, 5, 10, 25, 50, and 100 year; appendix figs. 2–4 through 2–9, respectively).
Determined by (1) georeferencing the precipitation contour images (Huff and Angel, 1992) for each recurrence interval to a coverage with known spatial reference and tracing the contour lines, (2) using the *Topo to Raster* tool from the ESRI ArcMap 9.3 3D Spatial Analyst Toolbox to interpolate to a raster, and (3) calculating the mean of each basin using zonal statistics (for small basins that were unable to be automatically calculated, values were estimated manually).

Climate factor (CT), (T = 2-, 25-, and 100-year recurrence intervals), identifies regional trends in small-basin flood frequency by incorporating long-term rainfall and pan evaporation information (Lichty and Karlinger, 1990).
The 2-year climate factor is shown in appendix figure 2–10.
Determined by (1) georeferencing the climate factor contour images (Lichty and Karlinger, 1990) for each recurrence interval to a coverage with known spatial reference information and tracing the contour lines, (2) using the topo to raster tool in the 3D Spatial Analyst Toolbox to interpolate a raster, and (3) calculating the mean of each basin using zonal statistics (for small basins that were unable to be automatically calculated, values were estimated manually).

Water, percentage of the basin classified as water: all areas of open water, generally with less than 20-percent cover of vegetation or soil.
Determined by (1) summing the areas of the 2011 National Land Cover Dataset (National Land Cover Dataset; https://www.mrlc.gov/data/nlcd-2001-land-cover-conus, accessed April 2020) grid cells contained within the basin classified as open water, and (2) dividing by the area of the basin and multiplying by 100.

Developed, percentage of the basin classified as developed. Determined by (1) summing the areas of the 2011 edition of the 2001 NLCD (https://www.mrlc.gov/data/nlcd-2001-land-cover-conus, accessed April 2020) grid cells contained within the basin classified as low, medium, or high intensity urban development (land-cover classes 22, 23, 24), and (2) dividing by the area of the basin and multiplying by 100.

Forest, percentage of the basin classified as forest. Determined by (1) summing the areas of the 2011 edition of the 2001 NLCD (https://www.mrlc.gov/data/nlcd-2001-land-cover-conus, accessed April 2020) grid cells contained within the basin classified as deciduous, evergreen, or mixed forest (land-cover classes 41, 42, 43), (2) dividing by the area of the basin and multiplying by 100.

HerbCult, percentage of the basin classified as pasture/hay or cultivated crops. Determined by (1) summing the areas of the 2011 edition of the 2001 NLCD (https://www.mrlc.gov/data/nlcd-2001-land-cover-conus, accessed April 2020) grid cells contained within the basin characterized by herbaceous vegetation that has been planted or is intensively managed for the production of food, feed, or fiber; or is maintained in developed settings for specific purposes (land-cover classes 81, 82), and (2) dividing by the area of the basin and multiplying by 100.

HerbNat, percentage of the basin classified as grassland/herbaceous: areas dominated by grammanoid or herbaceous vegetation, generally greater than 80-percent of total vegetation). Determined by (1) summing the areas of the 2011 edition of the 2001 NLCD (https://www.mrlc.gov/data/nlcd-2001-land-cover-conus, accessed April 2020) grid cells contained within the basin dominated by grammanoid or herbaceous vegetation (land-cover class 71), and (2) dividing by the area of the basin and multiplying by 100.

Wetland, percentage of the basin classified as soil/substrate that is periodically saturated or covered with water, containing more than 20 percent forest or shrub vegetation. Determined by (1) summing the areas of the 2011 edition of the 2001 NLCD (https://www.mrlc.gov/data/nlcd-2001-land-cover-conus, accessed April 2020) grid cells contained within the basin dominated by (land-cover classes 90, 95), and (2) dividing by the area of the basin and multiplying by 100.

Flood-Frequency Areas in Wisconsin

Because the State consists of diverse physiographic and climatic settings, dividing the State into somewhat homogeneous regions can result in regression equations with lower standard errors. In the last two versions of this report, the State was divided into five areas (Conger, 1981; Krug and others, 1992). For this report, the flood-frequency areas were revisited by using several alternative factors to define homogeneous areas. Variables considered included physiographic regions, major river-basin boundaries, surficial geology, and level 3 and 4 ecoregions (Omernik, 1987). A combination of level 3 ecoregions and major river basin boundaries resulted in reasonably homogeneous regions. The final flood-frequency areas are depicted in plate 1.

Areas 1–2 represent the Northern Lakes and Forests ecoregion, areas 3–4 fall within the North Central Hardwoods ecoregion, the Driftless Area is represented by areas 5–6, and the Southeast Till Plain is made up of areas 7–8. In all cases, the variability in the p-percent AEP floods was best explained by a different set of independent variables for each of the flood areas. For example, slope and forest cover were important for explaining the variability of floods in area 1, whereas the water land-use variable was important in area 2. Likewise, although the majority of the watersheds are rural, there is enough development within the basins in area 7 to warrant inclusion of the developed land-use variable in explaining the variability of floods, whereas saturated hydraulic conductivity and the water land-use variable were important for area 8.

Flood-Frequency Equations and Accuracy Evaluation

For this study, a combination of OLS and GLS regressions was used to determine the best-fit regression equations for each flood-frequency area (plate 1). A stepwise OLS procedure was used as a screening tool to determine the suite of variables that best predicted the flood associated with each p-percent AEP for each area. The stepwise procedure selects a subset of variables from a group of candidate basin characteristics (as described in the “Independent Variables” section) beginning with the variable that explains the most variability in the dependent variable, and continues with each successive variable that explains the most remaining variability given the effects of the variables already chosen. A variable was included if its coefficient was determined to be significantly different from zero at the 5-percent level (significance level less than 0.05).

For most areas, the stepwise procedure results in a slightly different set of independent variables for each of the p-percent AEP floods (50, 20, 10, 4, 2, 1, 0.5 and 0.2 percent). To maintain consistency, a common set of variables was chosen to predict each of the p-percent AEP floods in a particular area; in general, the set of variables explaining the most variability of the higher recurrence interval floods (1 and 0.5 percent) was chosen. This set of variables was then used to estimate the regressions using the GLS procedure. Selecting a set of variables that deviates from the stepwise results will produce a somewhat diminished accuracy of prediction for the regression. However, the increase in standard error for a common set of independent variables is likely compensated for by the improvements afforded by the GLS procedure.

The resulting influence statistics from the GLS regressions were examined to determine if the regressions could be improved by dropping selected streamflow-gaging stations.

The influence statistic is a measure of how influential a particular data point is to the overall regression equation, and is computed by comparing the regression with the full set of points to the regression calculated by dropping a particular point. Based on the total number of points available for a regression, a threshold can be determined that indicates when a particular data point has high influence on the resulting regression. For each regression, the streamflow-gaging station with high influence were examined in detail by looking at two factors: (1) how far the independent variables deviated from the average across all of the sites, and (2) the relative uncertainty in the estimate of the 1-percent AEP flood based on the crest-stage-gage uncertainty analysis described in appendix 1. If either the independent variables were extremely different than the mean values or if the uncertainty in the 1-percent AEP flood estimate was unusually high, the streamflow-gaging station was dropped from the regression. In all, five sites were dropped from the regressions (two in area 1, and one each in areas 2, 5, and 6). For these areas, the regressions were recomputed by using the reduced dataset.

The flood-frequency equations developed for streams in Wisconsin, along with the standard error of the model in percent, are presented in table 2. The most significant independent variables in the regression equations include drainage area, soil saturated hydraulic conductivity, main-channel slope, and several land-use variables. Interestingly, in area 3 drainage area is not one of the significant variables; it is included in all of the other areas. As a result, the multiplier coefficient at the beginning of each equation is considerably larger than the multipliers for the other areas. This is likely due to less variability in the two independent variables (slope and annual precipitation) compared to the variability in drainage area. The standard errors of estimate for area 3 are higher compared to the other areas, which could in part be due to a small sample size for this area (17 gages compared to 26–49 gages for the other areas). Further, there is an unusually high proportion of crest-stage gages in this area (11 out of 17 stations), which could be contributing to the increased uncertainty and lack of explanatory power for drainage area, as the records for crest-stage-gaging stations have a higher uncertainty compared to continuous-record streamflow-gaging stations and tend to be located on small headwater streams. For future reports it would be beneficial to develop regional equations jointly with Minnesota for basins that span the Minnesota-Wisconsin border, which would increase the number of sites available for the regression analysis.

The standard error of prediction, shown in table 2, is computed differently in this study, and the values are not directly comparable to previous studies (Conger, 1971; Conger, 1981; Krug and others, 1992; Walker and Krug, 2003). In general, the standard error of prediction is an average value across the set of independent variables, and is an indication of the relative uncertainty of an average prediction for any particular specific set of independent variable values. Overall, the standard errors of prediction are higher than those in previous reports (Ericson, 1961; Conger, 1971; Conger, 1981; Krug and others, 1992; and Walker and Krug, 2003). The increase in the standard errors of prediction is likely the result of the increased variability of the magnitude of the annual peak discharges at all of the sites.

Table 2. Flood-frequency equations for streams in Wisconsin.

[SEP, standard error of prediction; Q_{xp}, discharge for x-percent annual exceedance probability flood; A, drainage area, in square miles; S, main-channel slope, in feet per mile; K_{sat}, saturated hydraulic conductivity, in micrometers per second; LU_w, land use classified as water, (percent + 0.01)/100; LU_d, land use classified as developed, (percent + 0.01)/100; F, land use classified as forest, (percent + 0.01)/100]

Best-fit equation						SEP, in percent
Area 1, 35 streamflow-gaging stations						
Q_{50p}	=	0.546	$A^{1.03}$	$S^{0.906}$	$F^{-1.06}$	67.2
Q_{20p}	=	0.753	$A^{1.03}$	$S^{0.960}$	$F^{-1.04}$	63.4
Q_{10p}	=	0.893	$A^{1.03}$	$S^{0.993}$	$F^{-1.02}$	61.6
Q_{4p}	=	1.08	$A^{1.02}$	$S^{1.03}$	$F^{-0.983}$	58.5
Q_{2p}	=	1.22	$A^{1.02}$	$S^{1.06}$	$F^{-0.955}$	56.3
Q_{1p}	=	1.36	$A^{1.02}$	$S^{1.08}$	$F^{-0.931}$	55.0
$Q_{0.5p}$	=	1.50	$A^{1.02}$	$S^{1.11}$	$F^{-0.906}$	53.7
$Q_{0.2p}$	=	1.68	$A^{1.02}$	$S^{1.14}$	$F^{-0.876}$	51.7
Area 2, 31 streamflow-gaging stations						
Q_{50p}	=	3.18	$A^{0.922}$	$LU_w^{-0.205}$		47.7
Q_{20p}	=	3.99	$A^{0.918}$	$LU_w^{-0.235}$		56.2
Q_{10p}	=	4.54	$A^{0.915}$	$LU_w^{-0.250}$		60.3
Q_{4p}	=	5.28	$A^{0.913}$	$LU_w^{-0.264}$		64.5
Q_{2p}	=	5.89	$A^{0.910}$	$LU_w^{-0.272}$		67.7
Q_{1p}	=	6.47	$A^{0.909}$	$LU_w^{-0.280}$		70.2
$Q_{0.5p}$	=	7.11	$A^{0.907}$	$LU_w^{-0.286}$		72.8
$Q_{0.2p}$	=	7.98	$A^{0.904}$	$LU_w^{-0.293}$		76.9
Area 3, 17 streamflow-gaging stations						
Q_{50p}	=	51.6	$A^{0.700}$			61.4
Q_{20p}	=	94.2	$A^{0.670}$			70.7
Q_{10p}	=	129	$A^{0.655}$			76.7
Q_{4p}	=	181	$A^{0.639}$			84.3
Q_{2p}	=	225	$A^{0.630}$			90.7
Q_{1p}	=	273	$A^{0.621}$			97.4
$Q_{0.5p}$	=	327	$A^{0.614}$			104
$Q_{0.2p}$	=	405	$A^{0.605}$			114
Area 4, 45 streamflow-gaging stations						
Q_{50p}	=	1,760	$A^{0.709}$	$K_{sat}^{-1.22}$		54.0
Q_{20p}	=	3,620	$A^{0.691}$	$K_{sat}^{-1.29}$		58.1
Q_{10p}	=	5,280	$A^{0.680}$	$K_{sat}^{-1.33}$		60.1
Q_{4p}	=	7,930	$A^{0.669}$	$K_{sat}^{-1.37}$		62.2
Q_{2p}	=	10,300	$A^{0.662}$	$K_{sat}^{-1.40}$		62.8
Q_{1p}	=	13,100	$A^{0.656}$	$K_{sat}^{-1.42}$		63.5
$Q_{0.5p}$	=	16,200	$A^{0.650}$	$K_{sat}^{-1.44}$		64.2
$Q_{0.2p}$	=	21,000	$A^{0.643}$	$K_{sat}^{-1.47}$		65.6

Table 2. Flood-frequency equations for streams in Wisconsin.—Continued

[SEP, standard error of prediction; Q_{xp}, discharge for x-percent annual exceedance probability flood; A, drainage area, in square miles; S, main-channel slope, in feet per mile; K_{sat}, saturated hydraulic conductivity, in micrometers per second; LU_w, land use classified as water, (percent + 0.01)/100; LU_d, land use classified as developed, (percent + 0.01)/100; F, land use classified as forest, (percent + 0.01)/100]

Best-fit equation						SEP, in percent
Area 5, 26 streamflow-gaging stations						
Q_{50p}	=	183	$A^{0.701}$	$K_{sat}^{-0.540}$	$F^{-0.422}$	47.5
Q_{20p}	=	521	$A^{0.707}$	$K_{sat}^{-0.701}$	$F^{-0.403}$	45.4
Q_{10p}	=	951	$A^{0.709}$	$K_{sat}^{-0.796}$	$F^{-0.383}$	45.1
Q_{4p}	=	1,870	$A^{0.709}$	$K_{sat}^{-0.906}$	$F^{-0.358}$	46.0
Q_{2p}	=	2,950	$A^{0.710}$	$K_{sat}^{-0.982}$	$F^{-0.340}$	47.7
Q_{1p}	=	4,530	$A^{0.709}$	$K_{sat}^{-1.05}$	$F^{-0.316}$	48.5
$Q_{0.5p}$	=	6,750	$A^{0.709}$	$K_{sat}^{-1.12}$	$F^{-0.302}$	50.1
$Q_{0.2p}$	=	11,100	$A^{0.708}$	$K_{sat}^{-1.21}$	$F^{-0.277}$	51.1
Area 6, 37 streamflow-gaging stations						
Q_{50p}	=	0.282	$A^{1.25}$	$S^{1.01}$	$F^{-0.288}$	46.5
Q_{20p}	=	0.201	$A^{1.35}$	$S^{1.23}$	$F^{-0.308}$	43.9
Q_{10p}	=	0.190	$A^{1.38}$	$S^{1.32}$	$F^{-0.319}$	44.1
Q_{4p}	=	0.195	$A^{1.42}$	$S^{1.41}$	$F^{-0.330}$	46.3
Q_{2p}	=	0.203	$A^{1.43}$	$S^{1.46}$	$F^{-0.337}$	49.4
Q_{1p}	=	0.213	$A^{1.45}$	$S^{1.50}$	$F^{-0.343}$	53.6
$Q_{0.5p}$	=	0.226	$A^{1.46}$	$S^{1.54}$	$F^{-0.348}$	58.4
$Q_{0.2p}$	=	0.240	$A^{1.47}$	$S^{1.58}$	$F^{-0.355}$	66.1
Area 7, 49 streamflow-gaging stations						
Q_{50p}	=	137	$A^{0.642}$	$LU_d^{0.442}$		61.7
Q_{20p}	=	252	$A^{0.609}$	$LU_d^{0.447}$		67.3
Q_{10p}	=	347	$A^{0.594}$	$LU_d^{0.454}$		71.1
Q_{4p}	=	489	$A^{0.577}$	$LU_d^{0.465}$		75.6
Q_{2p}	=	610	$A^{0.568}$	$LU_d^{0.475}$		79.3
Q_{1p}	=	741	$A^{0.560}$	$LU_d^{0.485}$		83.3
$Q_{0.5p}$	=	889	$A^{0.552}$	$LU_d^{0.495}$		87.4
$Q_{0.2p}$	=	1,100	$A^{0.544}$	$LU_d^{0.509}$		93.1
Area 8, 44 gaging stations						
Q_{50p}	=	150	$A^{0.649}$	$K_{sat}^{-0.895}$	$LU_w^{-0.147}$	49.4
Q_{20p}	=	292	$A^{0.657}$	$K_{sat}^{-1.09}$	$LU_w^{-0.189}$	44.6
Q_{10p}	=	378	$A^{0.662}$	$K_{sat}^{-1.15}$	$LU_w^{-0.212}$	44.4
Q_{4p}	=	473	$A^{0.668}$	$K_{sat}^{-1.20}$	$LU_w^{-0.235}$	45.6
Q_{2p}	=	527	$A^{0.671}$	$K_{sat}^{-1.21}$	$LU_w^{-0.249}$	47.5
Q_{1p}	=	571	$A^{0.674}$	$K_{sat}^{-1.22}$	$LU_w^{-0.261}$	49.9
$Q_{0.5p}$	=	603	$A^{0.676}$	$K_{sat}^{-1.21}$	$LU_w^{-0.271}$	52.4
$Q_{0.2p}$	=	630	$A^{0.679}$	$K_{sat}^{-1.20}$	$LU_w^{-0.283}$	56.1

The percent change in coefficient of variation between the data through water year 2010 and the data through water year 2000 is shown in figure 2 for the four level 3 ecoregions in the State. The coefficient of variation, defined as the standard deviation divided by the mean, is a dimensionless representation of the variation in the annual peak discharges. With the exception of the Northern Highland Lakes and Forests ecoregion (areas 1 and 2), the coefficients of variation for the data through water year 2010 are considerably higher than those with data through water year 2000. These distributions are skewed towards positive values, as indicated by the mean exceeding the median, and a longer upper tail (the upper whisker of the box plot).

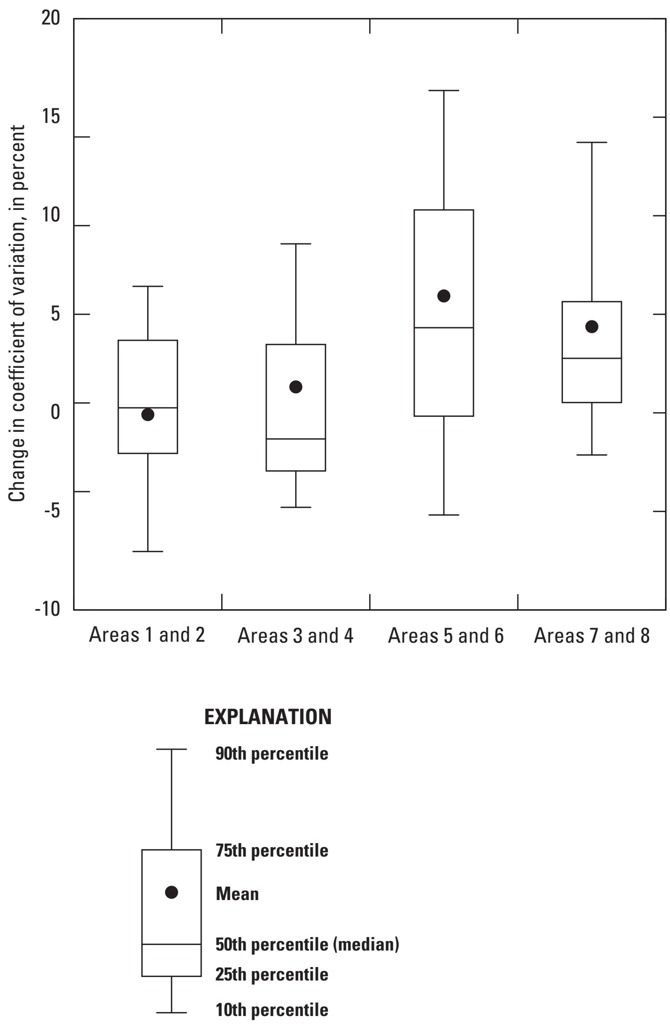

Figure 2. Change in coefficient of variation, in percent, computed with data through 2010 compared to coefficient of variation computed with data through 2000 for Northern Highlands Lakes and Forests (areas 1 and 2), for the North Central Hardwood Forests (areas 3 and 4), Driftless Area (areas 5 and 6) and Southeast Till Plain (areas 7 and 8).

The result of an overall increase in the variability of the annual peak discharges is reflected in an increase in flood magnitudes for higher frequencies (smaller p-percent AEP values). The percent change in discharge estimates for various AEP values between the data through water year 2010 and the data through water year 2000 is shown in figure 3 for the four level 3 ecoregions in the State. For all parts of the State, the distribution of the differences in flood magnitudes between the two periods for the two highest frequencies (2- and 1-percent AEP values) is skewed towards positive percent differences. The median and resulting distributions indicate an increase in the difference between data for the two periods as the frequency increases or the AEP decreases. Interestingly, for all of the level 3 ecoregions there is a decrease in the lower magnitude floods between the two periods. For some parts of the State, the differences in the 1-percent AEP floods between the two periods is quite large; for the Driftless Area and Southeast Till Plain (fig. 3, panels *C* and *D*, respectively), 90 percent of the sites had increases in the 1-percent AEP floods. In the Driftless Area, 10 percent of the sites had increases in the 1-percent AEP flood in excess of 40 percent.

One of the key assumptions in the log Pearson type III analysis is that the underlying annual-peak discharges are stationary, which means the parameters for the underlying probability distribution are unchanging with time. This translates to a requirement that the basic summary statistics for a site also are stationary. There is a growing body of evidence that streamflow records are not stationary (for example, Milly and others, 2008; and Gebert and Krug, 1996). The most likely causes of the nonstationarity in streamflow records are changes in land use and climate. To examine the likelihood of nonstationarity in the data used for the log Pearson type III analyses, the Mann Kendall statistic (Helsel and Hirsch, 2002) was computed for the nonregulated annual-peak discharges used in this report. The statistic can be used to test the null hypothesis that the data do not change with time against the alternate hypothesis that the values either increase or decrease monotonically with time. The sign of the test statistic (Kendall's τ) indicates the direction of the change (positive for increasing trend and negative for decreasing trend). The results of the trend tests are shown in appendix, table 2–1. Streamflow-gaging stations with a p-value less than 0.05 are considered to have a significant trend at the 5-percent level.

There is considerable evidence that there are significant trends in the annual-peak discharges used in this report. Overall, 28 sites have significant downward trends, 32 sites have significant upward trends, and 253 sites have no detectable trends. A detailed analysis of the likely cause of the trends is beyond the scope of this report. Further, developing techniques for including nonstationarity in flood-frequency analysis and regression analysis is an active area of research. Future frequency and regression analyses for the State need to incorporate techniques to include nonstationarity. It is believed that properly accounting for nonstationarity will reduce the overall uncertainty in the frequency estimates, which should result in less uncertain regional regression equations.

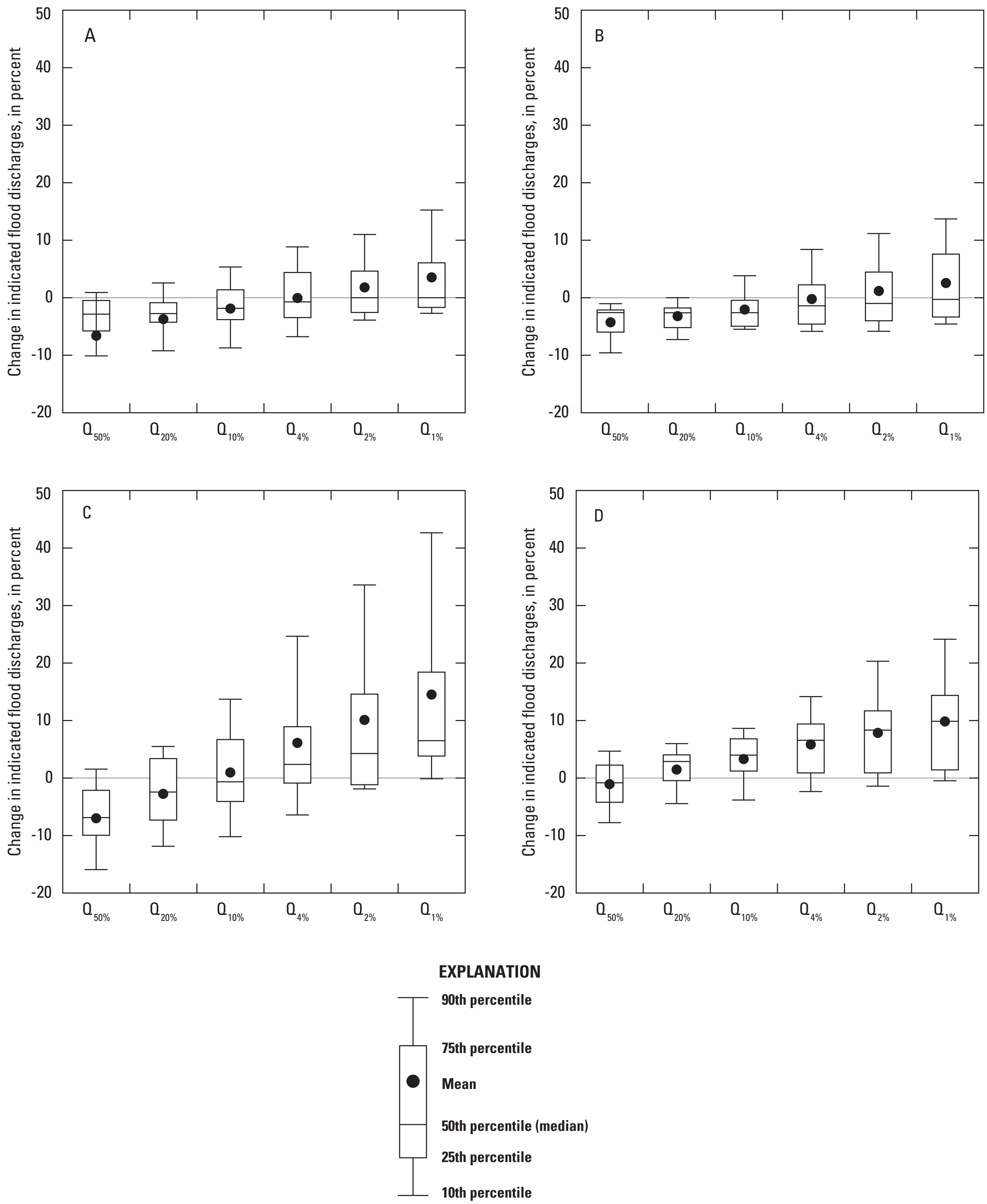

Figure 3. Change, in percent, in flood discharges computed with data through 2010 compared to flood discharges computed with data through 2000 for specific annual exceedance probabilities in *A*, Northern Highlands Lakes and Forests (areas 1 and 2); *B*, North Central Hardwood Forests (areas 3 and 4); *C*, Driftless Area (areas 5 and 6); and *D*, Southeast Till Plain (areas 7 and 8). Qx% represents the flood discharge corresponding to an annual exceedance of x-percent.

Techniques for Estimating Flood-Peak Discharges

The estimation techniques in this report can be applied to four types of rural sites. The first case is where the site is at a streamflow-gaging station; for this case, both Log Pearson type III and regression estimates are presented. The second case is where the site is near a streamflow-gaging station; for this case, the discharge from the appropriate regression equation is adjusted using information from the gaging record. The third case is where there is no streamflow-gaging station on the stream; for this case, the appropriate regression equation is applied directly. The fourth case is where the site is on a regulated stream; for this case, the discharge is estimated based on drainage area and the appropriate curve for the particular regulated stream (figs. 4–7). A detailed description for applying each technique is given in the examples that follow. To estimate flood frequencies for urban streams, the reader is referred to Conger (1986).

Streamflow-Gaging Stations

Flood-frequency characteristics of sites at streamflow-gaging stations can be estimated from the station streamflow record and by the regression equations. The two methods can be considered independent when a large number of sites were used to develop the regression equations. This is because the effect of a station on determining the regression equations is roughly inversely proportional to the number of stations used to determine the equations. Results for selected annual exceedance probabilities (AEP) from 50 to 0.2 percent are provided in the appendix, tables 2–1 through 2–9.

Sites Near Streamflow-Gaging Stations

Flood-frequency characteristics at sites near a streamflow-gaging station on the same stream are determined by using a combination of flood-frequency characteristics of the streamflow-gaging station and the characteristics determined by the regression equations. The procedure is applicable for sites that have a drainage area between 50 and 150 percent of the drainage area of the streamflow-gaging station. The suitability of the flood-frequency characteristics should be determined by comparing them with flood-frequency characteristics at the streamflow-gaging station. The following procedure was used by Curtis (1987) for streams in Illinois, based on work by Sauer (1974). The procedure is as follows:

First, the ratio r' is defined by

$$r' = \frac{Q_g}{\hat{Q}_g} - \left(\frac{\left|A_g - A_u\right|}{0.5A_g}\right)\left(\frac{Q_g}{\hat{Q}_g} - 1\right) \tag{2}$$

where

- r' is the adjustment ratio,
- Q_g is flood-frequency characteristics determined at the streamflow-gaging station,
- $\hat{Q}_g$ is flood-frequency characteristics determined for the streamflow-gaging station by the appropriate multiple-regression equation (from table 2),
- A_g is drainage area of gaged site, and
- A_u is drainage area of the ungaged site.

The adjusted flood-frequency characteristics for the ungaged site is computed by the equation

$$Q_u = r'\hat{Q}_u \tag{3}$$

where

- $\hat{Q}_u$ is flood-frequency characteristics determined for the ungaged site by the appropriate multiple-regression equation.

If the difference in drainage area between the ungaged site and the gaged site is more than 50 percent, equations 2 and 3 should not be used. In this case, the appropriate multiple-regression equation from table 2 should be used without adjustment but should be compared to the flood-frequency characteristics of the streamflow-gaging station on the stream for suitability. If the drainage area crosses the boundary of two flood-frequency areas, compute the flood frequency using equations from both areas. Compute the final flood-frequency estimates as the weighted average of the two estimates weighted by the proportion of drainage area in each of the flood-frequency areas.

Example: Determine the 1-percent AEP flood of Black Earth Creek at U.S. Highway 14 (not shown on plate 1), which is 2 miles downstream from the streamflow-gaging station Black Earth Creek at Black Earth (05406500); both sites are in area 6.

First, the appropriate equation from table 2 is used to determine the 1-percent AEP flood estimate at the gaged site:

$$Q_{1p} = 0.213A^{1.45}S^{1.50}F^{-0.343} \tag{4}$$

The drainage-basin characteristics at the gaged site are given in the appendix, table 2–11:

A = 44.1 mi^2,
S = 8.3, and
F = 34.2 percent

Substituting into equation 4,

$$\hat{Q}_g = 0.213(44.1)^{1.45}(8.3)^{1.50}(0.3421)^{-0.343} = 1{,}783$$

$\hat{Q}_u$ at the Black Earth Creek at U.S. Highway 14 can be determined at the ungaged site by use of equation 3 and the procedure that was used to determine $\hat{Q}_g$ at the streamflow-gaging station, as follows:

$$\hat{Q}_u = 0.213A^{1.45}S^{1.50}F^{-0.343} \quad (5)$$

The drainage-basin characteristics at the ungaged site were determined as follows:

A = 46.9 mi²,
S = 7.94, and
F = 33.95 percent

Substituting into equation 5,

$$\hat{Q}_u = 0.213(46.9)^{1.45}(7.94)^{1.50}(0.3396)^{-0.343} = 1{,}829$$

From table A–7, the 1-percent AEP flood at the streamflow-gaging station (Q_g) is 1,944. Next, equation 2 is used to determine the adjustment factor (r'):

$$r' = \frac{Q_g}{\hat{Q}_g} - \left(\frac{\left|A_g - A_u\right|}{0.5A_g}\right)\left(\frac{Q_g}{\hat{Q}_g} - 1\right)$$

$$r' = \frac{1{,}944}{1{,}783} - \left(\frac{\left|44.1 - 46.9\right|}{0.5 \times 44.1}\right)\left(\frac{1{,}944}{1{,}783} - 1\right) = 1.0788$$

Finally, equation 3 is used to compute the adjusted discharge at the ungaged site, thus

$$Q_u = r'\hat{Q}_u = 1.0788 \times 1{,}829 = 1{,}973$$

Sites Without Streamflow-Gaging Stations

Flood-frequency characteristics at sites on ungaged streams are calculated by using the appropriate equations from table 2. If the drainage area crosses the boundary of two flood-frequency areas, compute the flood frequency using equations from both areas. Compute the final flood-frequency estimates as the weighted average of the two estimates weighted by the proportion of drainage area in each of the flood-frequency areas.

Example: Determine the 1-percent AEP flood for Tappen Coulee at Blair (not shown on plate 1). This site is in area 5; therefore, the appropriate equation from table 2 is as follows:

$$Q_{1p} = 4{,}530A^{0.709}K_{sat}^{-1.05}F^{-0.316} \quad (6)$$

The drainage area A was determined to be 4.9 mi² by using the basin delineator tool (https://nhdplus.com/NHDPlus/NHDPlusV2_tools.php, accessed April 2020). The forest cover land-use variable (F) and mean hydraulic conductivity (K_{sat}) for the basin was calculated with the Zonal Statistics geoprocessing tool within Spatial Analyst in ArcGIS 10.1. Zonal Statistics tool calculates the mean value of a grid that falls within a zone, in this case, a drainage basin. This calculation results in a value of K_{sat} equal to 16.7 micrometers per second and a value of F equal to 32.4 percent.

Substituting these values into equation 6:

$$Q_{1p} = 4{,}530(4.9)^{0.709}(16.7)^{-1.05}(0.3241)^{-0.316} = 1{,}038$$

Regulated Streams

Flood-frequency characteristics at ungaged sites on regulated streams are estimated by using the flood-frequency characteristics at gaging stations on the regulated streams and adjusting the characteristics according to the relation of drainage area and discharge. Graphs showing the peak discharge of floods plotted at selected p-percent AEP values against drainage area are presented in figures 4–7 for the following major regulated streams in Wisconsin:

- Menominee River between Wisconsin and Michigan (fig. 4, not shown on plate 1),
- Wisconsin River from the mouth to Rainbow Reservoir near Lake Tomahawk (fig. 5, not shown on plate 1),
- Chippewa River from the mouth to Lake Chippewa in Sawyer County (fig. 6, not shown on plate 1), and
- Flambeau River from its mouth to Flambeau Flowage northeast of Park Falls (fig. 7, not shown on plate 1).

Storage reservoirs on the major regulated streams can substantially change the flood-frequency characteristics at gaging stations. Flood-frequency analyses were done for streamflow-gaging stations along the main stems for the period of record beginning with the completion of the last large storage reservoir in each basin. These analyses represent flood-frequency characteristics for the regulated period through 2010. The completion date for the reservoirs was 1941 for the Menominee River, 1926 for the Flambeau River, and 1923 for the Chippewa River. As discussed in the "Flood-Frequency Analysis" section, the peaks on the Wisconsin River before 1976 were modeled to reflect regulated conditions corresponding to conditions in 1977.

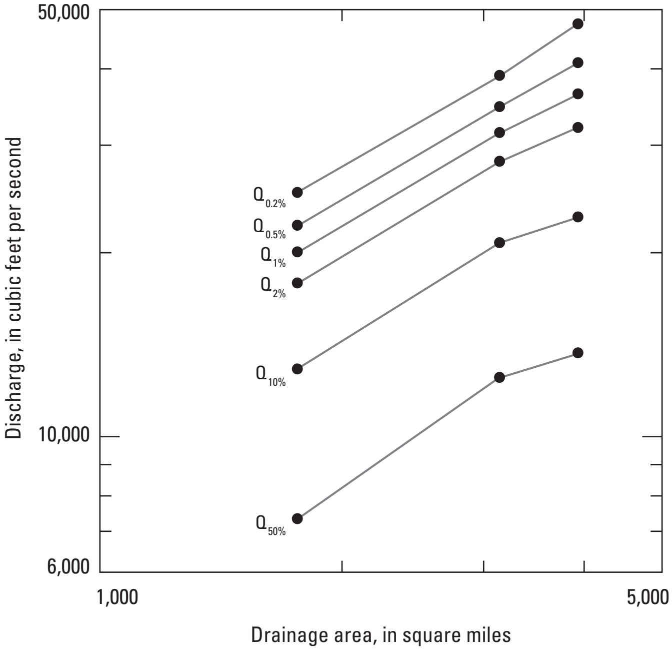

Figure 4. The relation of discharge to drainage area for selected flood frequencies along the main stem of the Menominee River, Wisconsin and Michigan. $Q_{x\%}$ represents the flood discharge corresponding to an annual exceedance of x-percent.

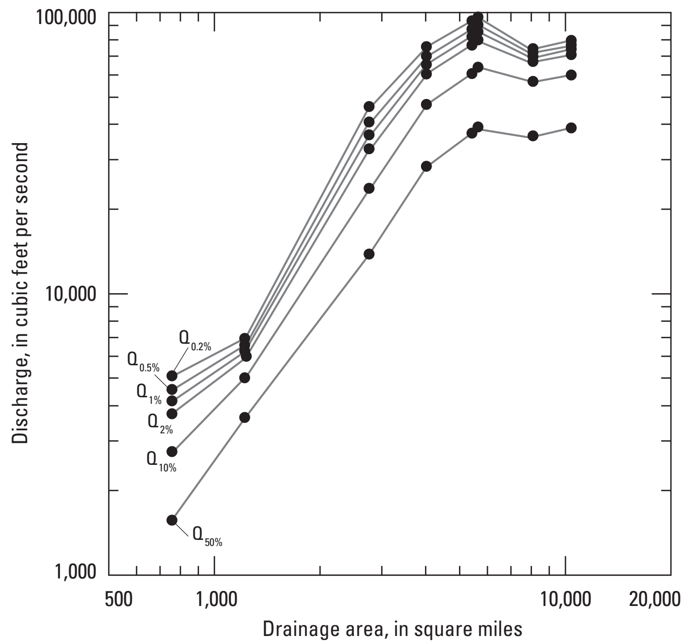

Figure 5. The relation of discharge to drainage area for selected flood frequencies along the main stem of the Wisconsin River. $Q_{x\%}$ represents the flood discharge corresponding to an annual exceedance of x-percent.

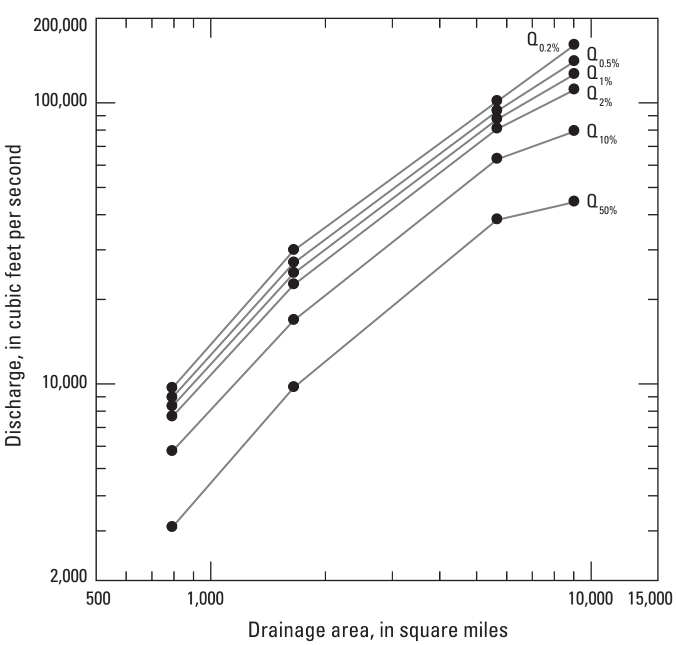

FIgure 6. The relation of discharge to drainage area for selected flood frequencies along the main stem of the Chippewa River. $Q_{x\%}$ represents the flood discharge corresponding to an annual exceedance of x-percent.

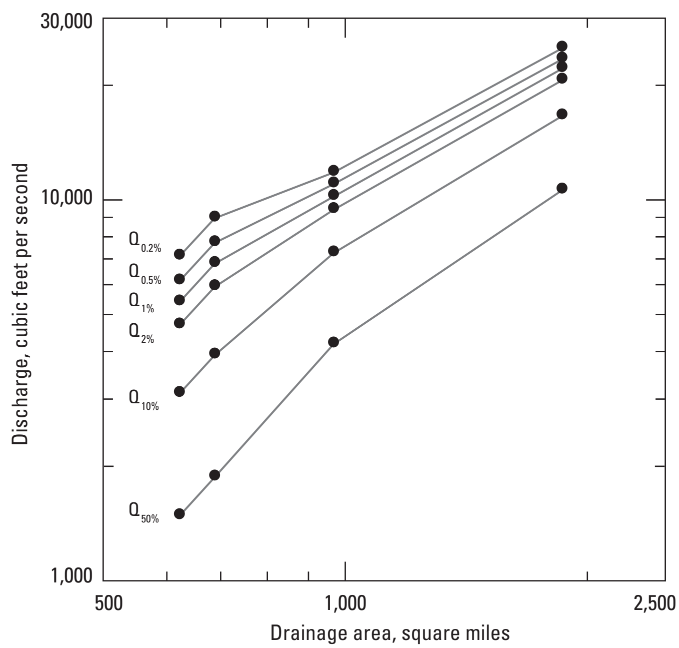

Figure 7. The relation of discharge to drainage area for selected flood frequencies along the main stem of the Flambeau River. $Q_{x\%}$ represents the flood discharge corresponding to an annual exceedance of x-percent.

Limitations of the Estimating Techniques

As mentioned previously, the regression equations presented in this report should only be applied to rural sites without substantial regulation. The regression equations and the associated accuracy are considered valid only within the area for which they were developed and within the range of basin-characteristic values used to calculate them. Flood estimates can be made using basin characteristics outside the range of values from which the equations were derived, but it is not possible to estimate the error in those values. The ranges of the basin characteristics of the gaging stations used in the regression analysis are summarized in table 3.

Table 3. Range of basin characteristics used in the regression analysis.

[mi^2, square miles; ft/mi, feet per mile; in., inches; µm/s, micrometers per second]

Basin characteristic	Minimum	Average	Maximum
Area 1, 35 streamflow-gaging stations			
Drainage area, mi^2	0.67	106	609
Main-channel slope, ft/mi	1.81	27.1	189
Land use, forest, percent	31.6	56.7	86.1
Area 2, 31 streamflow-gaging stations			
Drainage area, mi^2	1.67	137	1,120
Land use, water, percent	0	3.29	16.2
Area 3, 17 streamflow-gaging stations			
Drainage area, mi^2	1.37	243	1,100
Area 4, 45 streamflow-gaging stations			
Drainage area, mi^2	0.56	240	2,241
Saturated hydraulic conductivity, µm/s	8.96	25.1	71.3
Area 5, 26 streamflow-gaging stations			
Drainage area, mi^2	0.27	264	2,082
Saturated hydraulic conductivity, µm/s	6.63	22.9	63.4
Land use, forest, percent	13.0	39.3	67.9
Area 6, 37 streamflow-gaging stations			
Drainage area, mi^2	2.22	99.3	687
Main-channel slope, ft/mi	1.66	40.3	154
Land use, forest, percent	0.206	26.4	92.5
Area 7, 49 streamflow-gaging stations			
Drainage area, mi^2	0.82	481	6,344
Land use, developed, percent	1.13	13.42	86.48
Area 8, 44 streamflow-gaging stations			
Drainage area, mi^2	0.48	316	3,338
Saturated hydraulic conductivity, µm/s	62.7	75.5	111
Land use, water, percent	0.00	1.59	10.07

Summary

Equations, tables, and graphs presented in this report provide a means for estimating flood-frequency characteristics for unregulated rural streams and the major regulated streams in Wisconsin. For regulated streams, graphical relations of flood-frequency characteristics and drainage area are presented for the major regulated streams in Wisconsin: the Menominee, Flambeau, Chippewa, and Wisconsin Rivers. The relations were developed by use of data at streamflow-gaging stations for periods after the last large storage reservoir was constructed. For the Wisconsin River, the source of simulated flood discharges through 1976 was a report by Krug and House (1980). Observed flood discharges were used after 1976.

For unregulated streams, flood-frequency characteristics were determined at 154 crest-stage-gaging stations and 206 continuous-record streamflow-gaging stations using the log Pearson type III frequency distribution and a skewness map developed for the State. These characteristics, as well as drainage-basin characteristics, were used in a multiple-regression analysis to derive equations for estimating flood-frequency characteristics at ungaged sites. The generalized least-square procedure was used in the multiple-regression analyses. The State was divided into eight areas of similar physiographic characteristics. The most significant basin characteristics are drainage area, soil saturated hydraulic conductivity, main-channel slope, and several land-use variables. For each of the rural streamflow-gaging stations, weighted estimates based on the at-site log Pearson type III analysis and the regression results were determined. The weighted estimates generally have lower uncertainties than either the log Pearson type III or multiple regression estimates.

For the 1-percent annual exceedance probability (AEP) flood, the standard errors of prediction ranged from 56 to 70 percent. These values are higher than those reported in previous reports. The increase in the standard error of prediction is likely due to increased variability of the annual-peak discharges, resulting in increased variability in the magnitude of flood peaks at higher frequencies. This increase in variability may be due to nonstationarity in the discharge record coupled with the use of updated drainage-basin characteristics.

The regression equations and the associated accuracy are considered valid only within the area for which they were developed and within the range of basin-characteristic values used to calculate them.

References Cited

Cleveland, W.S., and Devlin, S.J., 1988, Locally weighted regression: An approach to regression analysis by local fitting: Journal of the American Statistical Association, v. 83, no. 403, p. 596–610.

Conger, D.H., 1971, Estimating magnitude and frequency of floods in Wisconsin: U.S. Geological Survey Open-File Report 91–2148, 200 p.

Conger, D.H., 1981, Techniques for estimating magnitude and frequency of floods for Wisconsin streams: U.S. Geological Survey Open-File Report 82–1214,, 115 p.

Conger, D.H., 1986, Estimating magnitude and frequency of floods for Wisconsin urban streams: U.S. Geological Survey Water-Resources Investigations Report 86–4005, 18 p.

Curtis, G.W., 1987, Technique for estimating flood-peak discharges and frequencies on rural streams: U.S. Geological Survey Water-Resources Investigations Report 87–4207, 79 p.

Eash, D.A., and Koppensteiner, B.A., 1997, Flood of July 9–11, 1993, in the Raccoon River basin, west-central Iowa: U.S. Geological Survey Open-File Report 97–557, 117 p.

Ericson, D.W., 1961, Floods in Wisconsin, magnitude and frequency: U.S. Geological Survey Open-File Report, 109 p.

Evergreen City Times, June 5, 1858, page 1 article.

Fitzpatrick, F.A., Peppler, M.C., Walker, J.F., Rose, W.J., Waschbusch, R.J., and Kennedy, J.L., 2008, Flood of June 2008 in Southern Wisconsin: U.S. Geological Survey Scientific Investigations Report 2008–5235, 24 p.

Flynn, K.M., Kirby, W.H., and Hummel, P.R., 2006, User’s manual for program PeakFQ, annual flood-frequency analysis using Bulletin 17B guidelines: U.S. Geological Survey Techniques and Methods 4–B4, 42 p.

Gebert, W.A., and Krug, W.R., 1996, Streamflow trends in Wisconsin’s driftless area: Journal of the American Water Resources Association, v. 32, no. 4, p. 733–744.

Helsel, D.R., and Hirsch, R.M., 2002, Statistical methods in water resources: U.S. Geological Survey Techniques of Water-Resource Investigations Report 04–A3, 523 p.

Huff, F.A., and Angel, J.R., 1992, Rainfall frequency atlas of the midwest: Illinois State Water Survey Bulletin 71, 148 p.

Interagency Advisory Committee on Water Data, 1982, Guidelines for determining flood flow frequency: U.S. Geological Survey, Office of Water Data Coordination Bulletin 17B of the Hydrology Subcommittee, 190 p.

Jarvis, Clarence S., and others, 1936, Floods in the United States: Magnitude and frequency: U.S. Geological Survey Water Supply Paper 771, 495 p.

Krug, W.R., Conger, D.H., and Gebert, W.A., 1992, Flood-frequency characteristics of Wisconsin streams: U.S. Geological Survey Water-Resources Investigations Report 91–4128, 185 p.

Krug, W.R., and House, L.B., l980, Streamflow model of Wisconsin River for estimating flood frequency and volume: U.S. Geological Survey Water-Resources Investigations Report 80–1103, 44 p.

Lichty, R.W., and Karlinger, M.R., 1990, Climate factor for small-basin flood frequency: Water Resources Bulletin, v. 26, no. 4, p. 577–586.

Lorenz, D.L., 1997, Generalized skew coefficients for flood-frequency analysis in Minnesota: U.S. Geological Survey Water-Resources Investigations Report 97–4089, 18 p.

Milly, P.C.D., Betancourt, J., Falkenmark, M., Hirsch, R.M., Kundzewicz, Z.W., Lettenmaier, D.P., and Stouffer, R.J., 2008, Stationarity is dead: Whither water management?: Science, v. 319, no. 5863, p. 573–574.

Omernik, J.M., 1987, Map supplement: Ecoregions of the conterminous United States: Annals of the Association of Amererican Geographers, v. 77, no. 1, p. 118–125.

Patterson, J.L., and Gamble, C.R., 1968, Magnitude and frequency of floods in the United States, part 5, Hudson Bay and Upper Mississippi River basins: U.S. Geological Survey Water-Supply Paper 1678, 546 p.

Sauer, V.B., 1974, Flood characteristics of Oklahoma streams: U.S. Geological Survey Water-Resources Investigations Report 52–73, 301 p.

Stedinger, J.R., and Tasker, G.D., 1985, Regional hydrologic analysis 1—Ordinary, weighted and generalized least squares compared: Water Resources Research, v. 21, no. 9, p. 1421–1432.

Tasker, G.D., Eychaner, J.H., and Stedinger, J.R., 1986, Application of generalized least squares in regional hydrologic regression analysis, *in* Subitzky, S., ed., Selected papers in the hydrologic sciences 1986: U.S. Geological Survey Water-Supply Paper 2310, p. 107–115.

The Baraboo Republic, March 17, 1859, page 1 article.

The Racine Daily Journal, June 13, 1899, page 1 article.

The Wisconsin State Journal, August 4, 1924, page 1 article.

University of Wisconsin-Madison, 2013, MadCat library catalog database, accessed June 2012, at http://madcat.library.wisc.edu/.

U.S. Geological Survey and others, 2012, Watershed Boundary Dataset for Wisconsin: accessed June 28, 2013, at http://datagateway.nrcs.usda.gov.

U.S. Geological Survey, 2013, National Water Information System (NWISWeb): U.S. Geological Survey database, accessed July, 2011, at http://dx.doi.org/10.5066/F7P55KJN.

Walker, J.F., and Krug, W.R., 2003, Flood-frequency characteristics of Wisconsin streams: U.S. Geological Survey Water-Resources Investigations Report 03–4250, 37 p.

Wiitala, S.W., 1965, Magnitude and frequency of floods in the United States, part 4, St. Lawrence River basin: U.S. Geological Survey Water-Supply Paper 1677, 357 p.

Wisconsinheritage.org, 2013, Wisconsin Library Services: Recollection Wisconsin program database, accessed June 2012, at http://recollectionwisconsin.org/.

Wisconsin Rapids Daily Tribune, April 6, 1959, page 1 article.

Wisconsin State Historical Society, 2013, Wisconsin Local History & Biography Articles: Wisconsin State Historical Society database, accessed June 2012, at http://www.wisconsinhistory.org/wlhba/.

Wisconsin State Historical Society, 2013, Access Newspaper ARCHIVE: BadgerLink database access, accessed June 2012, at http://access.newspaperarchive.com/.

Appendix 1. Crest-Stage Gage Uncertainty Analysis

There are two sources of uncertainty in the peak-discharge record generated at a crest-stage gage: the measurement of peak gage height, and the translation of peak stage to peak discharge through the rating curve. Crest-stage gages are visited periodically during the year, often several days or weeks following a high-streamflow event. As a result, the estimate of peak gage height will likely be more uncertain than a peak gage height from a continuous-record gage. As with continuous-record gages, rating curves for crest-stage gages are developed from periodic discharge measurements. Crest-stage gages tend to be installed in smaller watersheds with a very quick hydrologic response. Because crest-stage gaging stations do not have equipment that can report real-time gage heights, it is difficult to be at the site during high-streamflow events. As a result there are fewer discharge measurements to define the upper end of the rating curve and document temporary deviations (shifts) from the rating. Overall, one would expect the uncertainty in discharge from a crest-stage gage rating curve to be higher than the uncertainty in discharge from a continuous-record gage.

The overall uncertainty in the stage-discharge rating is a function of the number of discharge measurements used to define the rating and the uncertainty in the individual discharge measurements. Uncertainty in individual measurements was represented by a multiplicative log-normal error model (for example, Walker, 1981; Potter and Walker, 1982; Potter and Walker, 1985; Walker, 1985). Consider the following representation of error for a particular discharge measurement:

$$\hat{Q}_m = Q_m \eta \tag{1}$$

where Q_m is the true discharge, $\hat{Q}_m$ is the measured discharge, and η is the multiplicative error associated with the discharge measurement. If we assume η is log-normally distributed, then a log transformation of equation 1 results in an additive model, thus:

$$\log \hat{Q}_m = \log Q_m + \varepsilon \tag{2}$$

where ε is equal to $\log(\eta)$. Because η is log-normally distributed, ε is normally distributed. If we assume the discharge measurement is unbiased (that is, $E[\eta] = 1$) and has a discharge measurement error variance given by σ^2, the relation between real-space and log-space moments for the log-normal distribution (Miller and Freund, 1977) can be used to write the log-space mean (α) and variance (β^2) of the measurement error as follows:

$$\alpha = -\tfrac{1}{2}\log(1+\sigma^2) \tag{3}$$

$$\beta^2 = \log(1+\sigma^2) \tag{4}$$

The overall rating uncertainty was evaluated using a Monte Carlo framework (Miller and Freund, 1977). With the Monte Carlo approach, variables in the process that contain uncertainty are represented by probability distributions. The Monte Carlo experiment uses random samples from the assumed distributions as representative realizations of the process. The individual realizations are then summarized to provide estimates of the resulting process variables. For a particular site, measurement uncertainty was added to the individual discharge measurements used to develop the rating relation. The measurement uncertainty was estimated based on the rating assigned to the measurement; the standard U.S. Geological Survey rating scheme (excellent, good, fair, poor) was translated to an error standard deviation (σ_m: 0.025, 0.05, 0.7, 0.12) based loosely on typical uncertainties reported in the literature (Sauer and Meyer, 1992). The log-space error mean and variance were computed by setting $\sigma^2 = \sigma_m^2$ in equations 3 and 4, respectively. For each set of measurements, one or more rating curve segments were estimated using standard regression techniques (as much as three rating curve segments were estimated based on the break points and offsets used at a particular site). For a particular gage height, discharge estimates were made for each selected gage height based on the fitted rating curve and randomly generated errors. The Monte Carlo experiment results in the expected value and variance of the log of the rated discharges for a series of selected gage heights. The expected value and variance for a selected gage height can be written as two functions, namely:

$$\Psi_1(Ght) = E\left[\log Q_r\right] \tag{5}$$

$$\Psi_2(Ght) = V\left[\log Q_r\right] \tag{6}$$

The two functions defined by equations 5 and 6 represent the mean and variance of the log of discharge resulting from the uncertainty of the discharge measurements and the fitted rating curve for each selected gage height. The Monte Carlo experiment is summarized as follows:

1–1. Compute log-space moments for discharge measurement errors using equations 3 and 4 with $\sigma^2 = \sigma_m^2$

1–2. Set target gage height to minimum recordable gage height

1–3. Generate N_{meas} discharge measurement errors: $\varepsilon \sim N\left(\alpha_m, \beta_m^2\right)$

1–4. Compute measured discharges from equation 2

1–5. Compute new rating segments using perturbed measurements: $\log \hat{Q}_m = \beta_0 + \beta_1 \log\left(Ght_m - \text{offset}\right)$

1–6. Compute flow for target gage height from rating segments

1–7. Repeat steps 3–6 NR times. Compute statistics:

$$E\left[\log\hat{Q}\right]=\frac{1}{NR}\sum_{NR}\log\hat{Q}$$

$$V\left[\log\hat{Q}\right]=\frac{1}{NR}\sum_{NR}\left(\log\hat{Q}-\log Q\right)^2$$

1–8. Increment target gage height by 0.1 foot, and repeat steps 3–7 until target gage height exceeds maximum recordable gage height. Result is a lookup table, which can be used to estimate expected value and variance of discharge for a specified gage height.

A second Monte Carlo experiment was used to determine the uncertainty in peak discharge obtained from the rating curve and a measurement of peak gage height with inherent uncertainty. As with the discharge measurements, we assume an additive error model in log space for peak gage height. Thus an estimate of the log of gage height for a given “true” gage height is given by the following:

$$\log\widehat{Ght}=\log Ght+\omega \tag{7}$$

where $\widehat{Ght}$ is the estimated gage height, Ght is the true gage height, and ω is a normally distributed measurement error. For an unbiased error model in real space with error variance equal to σ_s^2, the log-space error mean and variance are computed using equations 3 and 4 by setting $\sigma^2=\sigma_s^2$.

For a particular estimated annual peak gage height, the estimated annual peak discharge in log space is given as follows:

$$\log\hat{Q}_p=\Psi_1(\widehat{Ght})+\gamma \tag{8}$$

where $\hat{Q}_p$ is the predicted annual peak discharge, $\Psi_1(\widehat{Ght})$ is the rating-curve function that gives the expected value of the log of discharge, and γ is the uncertainty in the predicted discharge because of uncertainty in the rating curve. For an unbiased real-space rating-curve error model, the mean and variance of γ are a function of the rating curve variance function evaluated at the estimated gage height, namely $\Psi_2(\widehat{Ght})$.

The true value of the annual peak discharge is obtained using the expected value function of the rating relation evaluated at the true gage height, thus:

$$\log Q_p=\Psi_1(Ght) \tag{9}$$

where Q_p is the true annual peak discharge, Ght is the true annual peak gage height, and $\Psi_1()$ is the expected value rating curve function. For a particular Monte Carlo experiment with N_{real} realizations, the mean-squared error (mse) of uncertainty in the log of peak discharge is given as:

$$mse\left(\log Q_p\right)=\sum_{NR}\left(\log Q_p-\log\hat{Q}_p\right)^2 \tag{10}$$

The real-space error standard deviation can be written by setting $\beta^2 = mse(\log Q_p)$ in equation 4 and solving for σ. The Monte Carlo experiment is summarized as follows:

2–1. Compute log-space moments for peak gage-height measurement error using equations 3 and 4 with $\sigma^2=\sigma_s^2$

2–2. Generate peak gage-height measurement error: $\omega\sim N\left(\alpha_s,\beta_s^2\right)$

2–3. Compute perturbed peak gage height $\log\widehat{Ght}=\log Ght+\omega$

2–4. Compute log-space moments for rating curve based on uncertainty of rating curve error

2–5. Generate log discharge rating error: $\gamma\sim N\left(\alpha_p,\beta_p^2\right)$

2–6. Compute the log of the rated discharge using equation 8

2–7. Repeat steps 2–6 NR times. Compute mean-squared error (mse) of log Q_p as:

$$mse\left[\log Q_p\right]=\frac{1}{NR}\sum_{NR}\left(\log\hat{Q}_p-\log Q_p\right)^2$$

Results

Based on a review of the record and site conditions, information was gathered to allow for an assessment of uncertainty in the 1-percent annual exceedance probability (AEP) flood for selected crest-gage sites. First, the current rating and the associated discharge measurements used to define the rating were determined. For each discharge measurement, the rated accuracy from the field notes (excellent, good, fair, poor) was used to assign an uncertainty associated with each measurement. Next, the breakpoints and offsets were used to define each rating-curve segment to be used in the first Monte Carlo experiment. Finally, an uncertainty in the annual peak gage height (σ_s) was assigned to each crest-stage gage site based on an interview with the hydrologic technician who works the record for a particular site. Criteria used to assign the peak gage-height uncertainty included stability of the gage datum, consistency and quality of readings, and frequency of visits. Although the assessment of the uncertainty in the peak gage height was qualitative, indications were that the relative uncertainty between crest-stage gages was probably captured reasonably well.

For each site, the discharge measurements used to define the current rating curve were used to define the expected value equation 5 and variance functions equation 6 as lookup tables using the procedure outlined in the first Monte Carlo experiment (steps 1–1 through 1–8 as listed in the previous section) and for gage heights ranging from the minimum to maximum recordable value.

For each site, the gage height corresponding to the 1-percent AEP flood was determined, and the procedure outlined in the second Monte Carlo experiment (steps 2–1 through 2–7 as listed in the previous section) was used to determine the mean-squared error of the log of the 1-percent AEP flood and the corresponding real-space coefficient of variation of the uncertainty in the 1-percent AEP flood.

The results from the second Monte Carlo experiment for selected crest-stage gages are given in table 1–1. Note that the results only include crest-stage gages that were operated during the 2010 water year (the period from October 1, 2009 through September 30, 2010); for discontinued gages there was not sufficient information available to complete the uncertainty analysis. Further, for a considerable number of gages the analysis resulted in unreasonably high estimates of uncertainty for the 1-percent AEP flood, so those analyses were dropped. The most likely causes for these cases were (1) a limited number of discharge measurements for one or more of the rating curve segments, (2) a lack of measurements at the upper end of the rating, and (3) highly uncertain discharge measurements with a rating of fair or poor. All of these symptoms would result in substantial extrapolation of an uncertain rating curve to provide an estimate of the 1-percent AEP flood.

In many cases, modest uncertainties in annual peak gage height (for example, less than 0.05) translate to modest uncertainties in the 1-percent AEP flood (for example, less than 0.1). However, there are many instances where the uncertainty in the 1-percent AEP flood is quite high (greater than 0.4) despite reasonable values for the uncertainty in the annual peak gage height. The likely cause of these high uncertainties in discharge is a lack of discharge measurements at the upper end of the rating curve. A secondary cause would be high levels of uncertainty in the discharge measurements, particularly at the high end of the rating. For crest-stage gaging stations with high uncertainties in the 1-percent AEP flood (mse[logQ] column in table 1–1), the ratings and measurements were examined in detail to set priorities for future discharge measurements at these sites.

Table 1–1. Estimates of peak gage-height error, mean-squared-error of log-transformed discharge, and associated coefficient of variation of error for untransformed discharge for the 1-percent annual exceedance probability flood for selected crest-stage gages in the Wisconsin flood-frequency network.

[USGS, U.S. Geological Survey; Wis., Wisconsin; mse, mean-squared error; Q, discharge in cubic feet per second; CV, coefficient of variation]

Area	USGS station number	Station name	Peak gage-height error	mse[logQ]	CV[Q]
1	04024400	Stoney Brook near Superior, Wis.	0.050	0.005	0.070
1	04026300	Sioux River near Washburn, Wis.	0.075	0.170	0.430
1	04026450	Bad River near Mellen, Wis.	0.030	0.010	0.100
1	04027200	Pearl Creek at Grandview, Wis.	0.100	0.086	0.300
2	04059900	Allen Creek Tributary near Alvin, Wis.	0.050	0.047	0.220
2	04067760	Peshtigo River near Cavour, Wis.	0.075	0.006	0.080
2	04069700	North Branch Oconto River near Wabeno, Wis.	0.040	0.047	0.220
4	04071700	North Branch Little River near Coleman, Wis.	0.100	0.006	0.080
4	04071800	Pensaukee River near Pulaski, Wis.	0.100	0.002	0.050
4	04072792	Tagatz Creek near Westfield, Wis.	0.025	0.408	0.710
4	04073400	Bird Creek at Wautoma, Wis.	0.050	0.008	0.090
2	04075200	Evergreen Creek near Langlade, Wis.	0.100	0.008	0.090
7	04085145	Red River at Ct Highway A near Dyckesville, Wis.	0.100	0.028	0.170
7	04087200	Oak Creek near South Milwaukee, Wis.	0.025	0.012	0.110
7	04087250	Pike Creek near Kenosha, Wis.	0.025	0.008	0.090
3	05340300	Trade River near Fredric, Wis.	0.050	0.006	0.080
3	05341313	Bull Brook at Cnty Trnk Highway F near Amery, Wis.	0.050)	0.070	0.270
5	05341900	Kinnickinnic River Trib at River Falls, Wis.	0.100	0.116	0.350
1	05357360	Bear River near Powell, Wis.	0.050	0.065	0.260
1	05359600	Price Creek near Phillips, Wis.	0.050	0.035	0.190
1	05361400	Hay Creek near Prentice, Wis.	0.050	0.006	0.080
1	05361420	Douglas Creek near Prentice, Wis.	0.050	0.075	0.280
1	05361989	Jump River Tributary near Jump River, Wis.	0.050	0.215	0.490

Table 1–1. Estimates of peak gage-height error, mean-squared-error of log-transformed discharge, and associated coefficient of variation of error for untransformed discharge for the 1-percent annual exceedance probability flood for selected crest-stage gages in the Wisconsin flood-frequency network.—Continued

[USGS, U.S. Geological Survey; Wis., Wisconsin; mse, mean-squared error; Q, discharge in cubic feet per second; CV, coefficient of variation]

Area	USGS station number	Station name	Peak gage-height error	mse[logQ]	CV[Q]
1	05363775	Babit Creek at Gilman, Wis.	0.050	0.008	0.090
3	05364000	Yellow River at Cadott, Wis.	0.100	0.056	0.240
1	05364100	Seth Creek near Cadott, Wis.	0.050	0.170	0.430
3	05366500	Eau Claire River near Fall Creek, Wis.	0.020	0.122	0.360
1	053674588	Rock Creek Tributary near Canton, Wis.	0.050	0.004	0.060
3	05367700	Lightning Creek at Almena, Wis.	0.060	0.389	0.690
5	05371920	Buffalo River near Mondovi, Wis.	0.050	0.371	0.670
5	05379288	Bruce Valley Creek near Pleasantville, Wis.	0.025	0.004	0.060
4	05380900	Poplar River near Owen, Wis.	0.050	0.008	0.090
5	05382200	French Creek near Ettrick, Wis.	0.025	0.135	0.380
2	05392150	Mishonagon Creek near Woodruff, Wis.	0.050	0.002	0.050
2	05392350	Bearskin Creek near Harshaw, Wis.	0.050	0.012	0.110
2	05393640	Little Pine Creek near Irma, Wis.	0.050	0.047	0.220
4	05394200	Devil Creek near Merrill, Wis.	0.100	0.014	0.120
4	05397600	Big Sandy Creek near Wausau, Wis.	0.100	0.019	0.140
4	05400025	Johnson Creek near Knowlton, Wis.	0.050	0.025	0.160
4	05401800	Yellow River Tributary near Pittsville, Wis.	0.025	0.075	0.280
6	05403700	Dell Creek near Lake Delton, Wis.	0.025	0.019	0.140
6	05406605	Lowery Creek near Spring Green, Wis.	0.050	0.017	0.130
6	05407039	Fennimore Fork near Fennimore, Wis.	0.075	0.019	0.140
6	05407200	Crooked Creek near Boscobel, Wis.	0.050	0.008	0.090
8	05425806	Mud Creek near Danville, Wis.	0.075	0.002	0.040
8	05436200	Gill Creek near Brooklyn, Wis.	0.050	0.010	0.100
8	05545100	Sugar Creek at Elkhorn, Wis.	0.025	0.070	0.270
8	05545200	White River Tributary near Burlington, Wis.	0.025	0.399	0.700
8	05548150	North Br Nippersink Creek near Genoa City, Wis.	0.025	0.022	0.150

Literature Cited

Miller, I., and Freund, J.E., 1977, Probability and statistics for engineers, second edition: Englewood Cliffs, N.J., Prentice-Hall, Inc., 529 p.

Potter, K.W., and Walker, J.F., 1982, Modeling the error in flood discharge measurements, *in* Shaarawi, A.H., and Esterby, S.W., eds., Developments in water science, v. 17, Time series methods in hydroscience: Amsterdam, Netherlands, Elsevier Scientific Publishing Company, p. 405–413.

Potter, K.W., and Walker, J.F., 1985, An empirical study of flood measurement error: Water Resources Research, v. 21, no. 3, p. 403–406.

Sauer, V.B., and Meyer, R.W., 1992, Determination of error in individual discharge measurements: U.S. Geological Survey Open-File Report 92–144, 21 p.

Walker, J.F., 1981, The impact of measurement error on the probability distribution of measureed flood discharges: Madison, University of Wisconsin, M.S. thesis, 95 p.

Walker, J.F., 1985, The impact of measurement error on the at-site flood frequency problem: Madison, University of Wisconsin, Ph.D. thesis, 207 p.

Appendix 2. Supporting Tables and Figures

Tables 2–1 through 2–11 are available for download from https://doi.org/10.33/sir20165140.

Table 2–1. General characteristics of the unregulated streamflow-gaging stations in the Wisconsin flood-frequency network.

Table 2–2. Discharges for the 50-percent annual exceedance probability floods for streamflow-gaging stations in the Wisconsin flood-frequency network.

Table 2–3. Discharges for the 20-percent annual exceedance probability floods for streamflow-gaging stations in the Wisconsin flood-frequency network.

Table 2–4. Discharges for the 10-percent annual exceedance probability floods for streamflow-gaging stations in the Wisconsin flood-frequency network.

Table 2–5. Discharges for the 4-percent annual exceedance probability floods for streamflow-gaging stations in the Wisconsin flood-frequency network.

Table 2–6. Discharges for the 2-percent annual exceedance probability floods for streamflow-gaging stations in the Wisconsin flood-frequency network.

Table 2–7. Discharges for the 1-percent annual exceedance probability floods for streamflow-gaging stations in the Wisconsin flood-frequency network.

Table 2–8. Discharges for the 0.5-percent annual exceedance probability floods for streamflow-gaging stations in the Wisconsin flood-frequency network.

Table 2–9. Discharges for the 0.2-percent annual exceedance probability floods for streamflow-gaging stations in the Wisconsin flood-frequency network.

Table 2–10. Discharges for selected p-percent annual exceedance probability floods and Water Resources Council estimated statistics for regulated streamflow-gaging stations in the Wisconsin flood-frequency network.

Table 2–11. Drainage-basin characteristics for rural streamflow-gaging stations in Wisconsin.

Figures 2–1 through 2–10 follow this page.

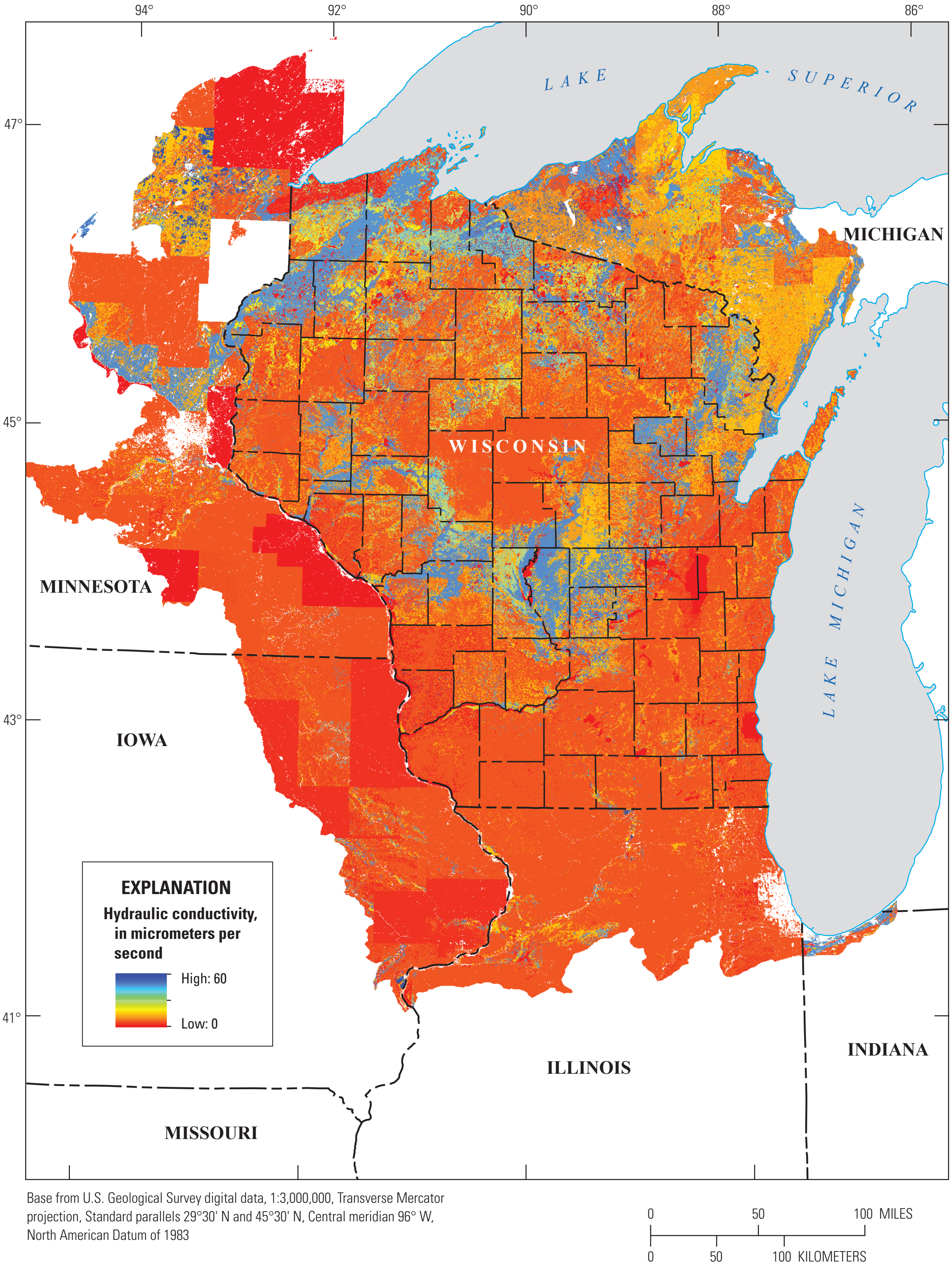

Figure 2–1. Distribution of saturated hydraulic conductivity across Wisconsin.

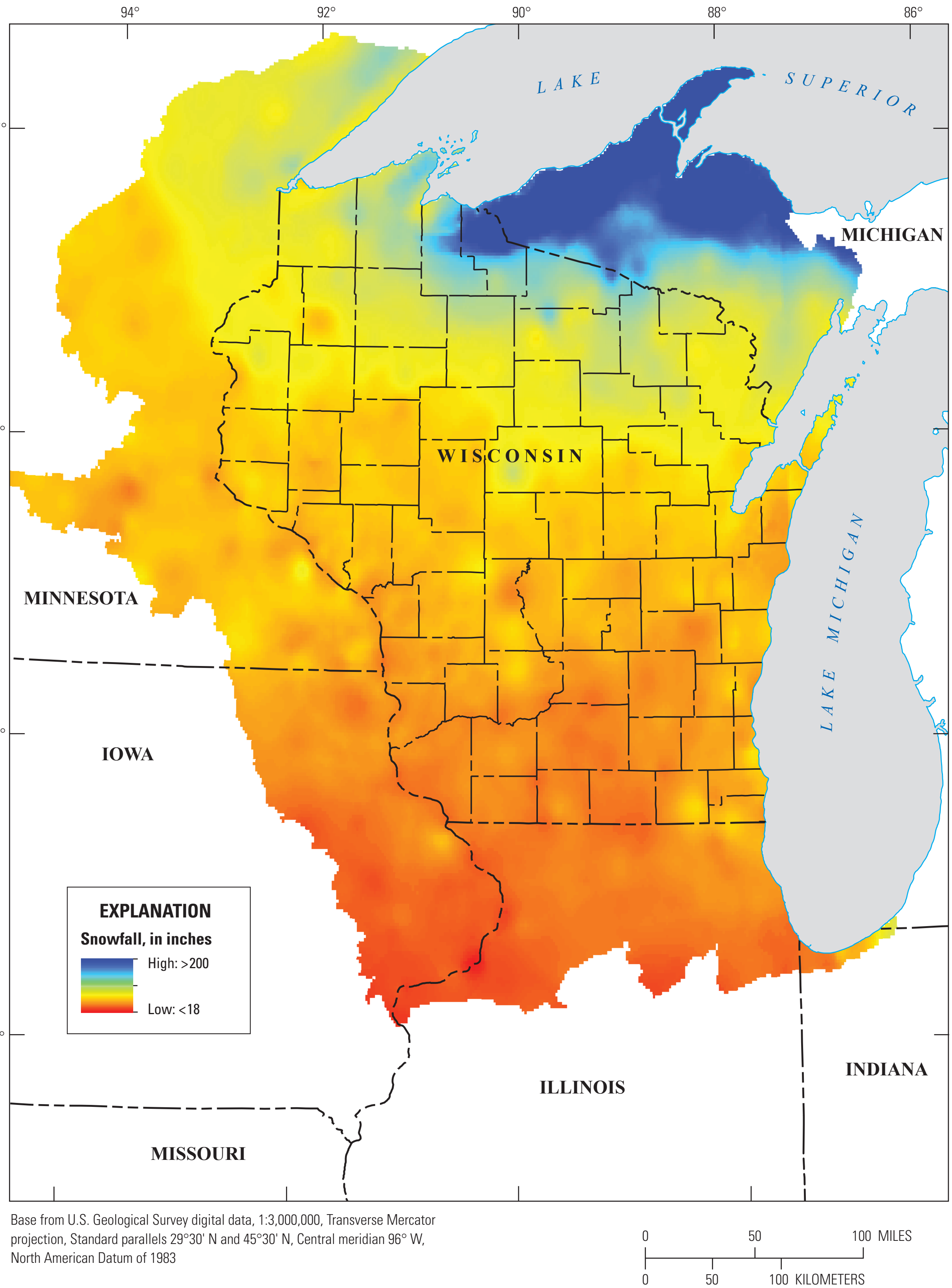

Figure 2–2. Distribution of annual snowfall across Wisconsin.

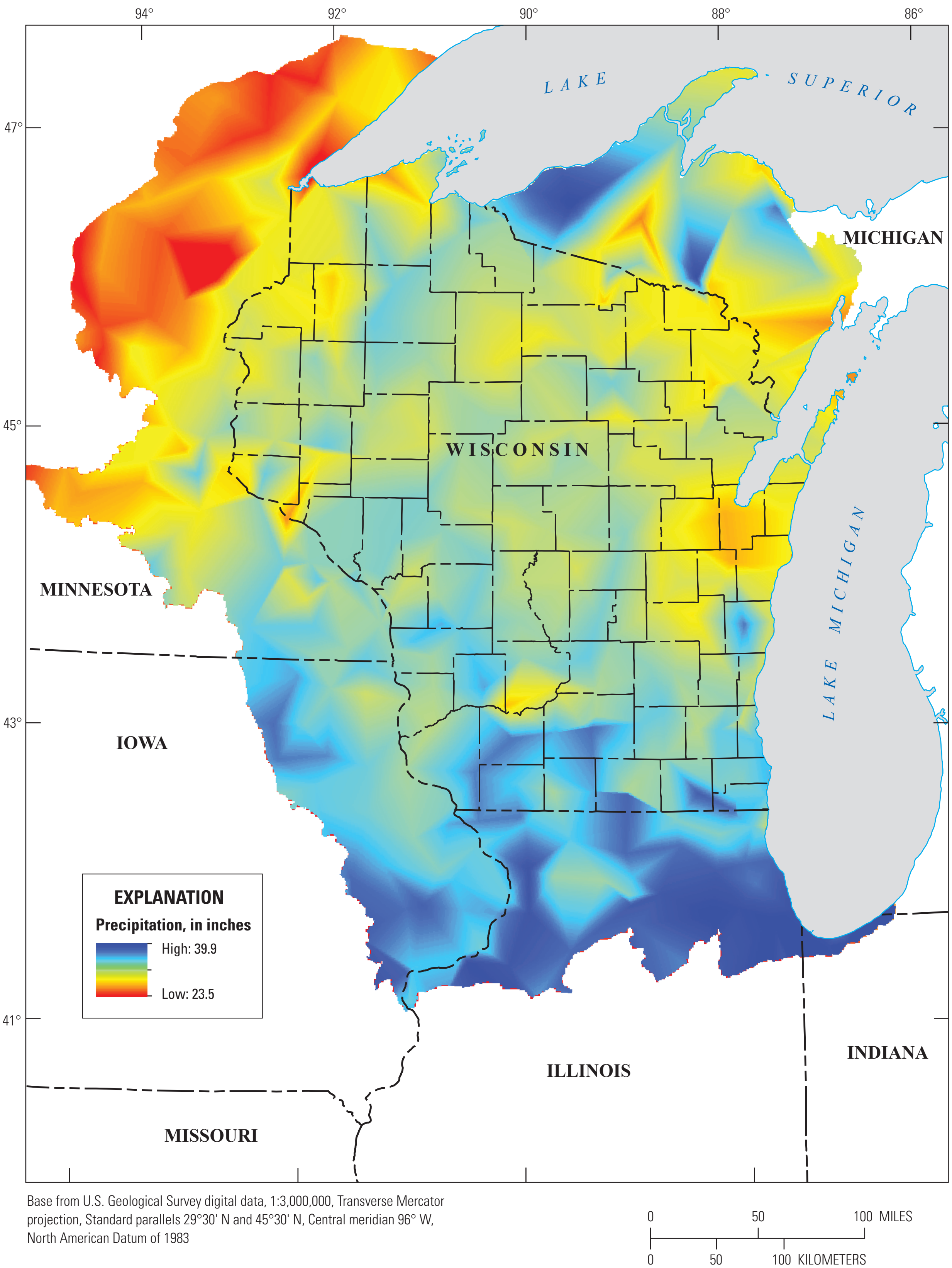

Figure 2–3. Distribution of annual precipitation across Wisconsin.

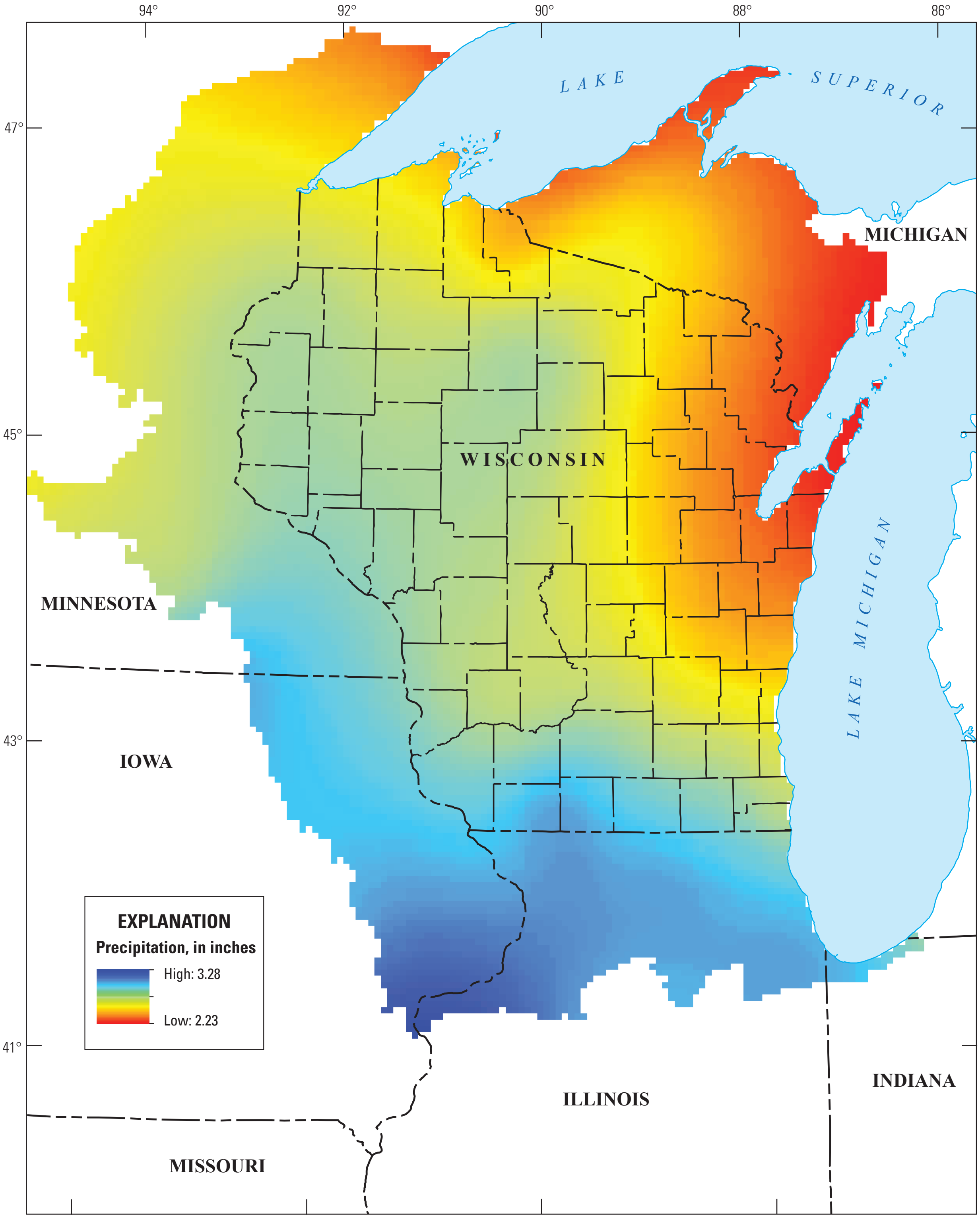

Base from U.S. Geological Survey digital data, 1:3,000,000, Transverse Mercator projection, Standard parallels 29°30' N and 45°30' N, Central meridian 96° W, North American Datum of 1983

0 50 100 MILES
0 50 100 KILOMETERS

Figure 2–4. Distribution of 2-year, 24-hour precipitation across Wisconsin.

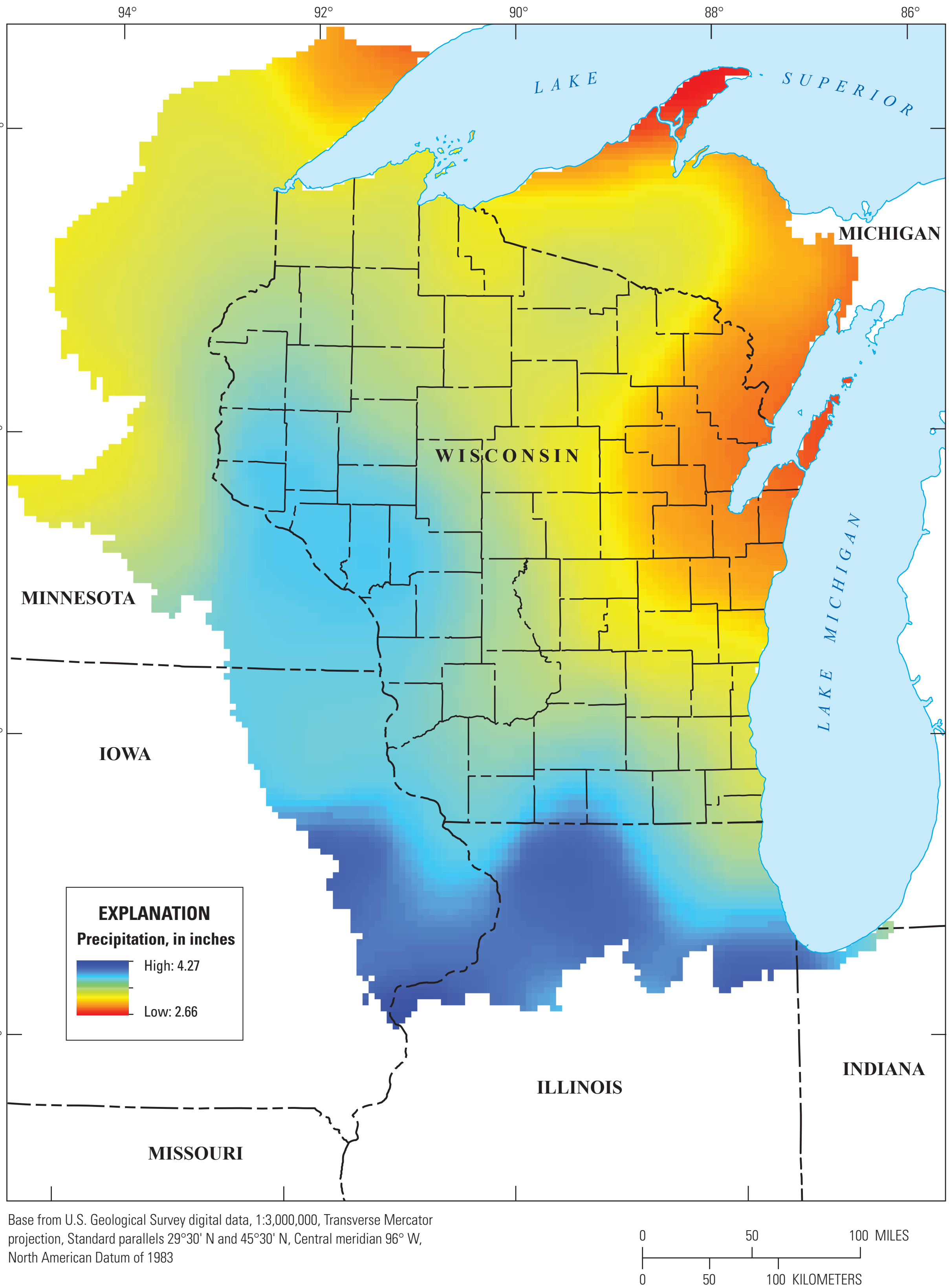

Figure 2–5. Distribution of 5-year, 24-hour precipitation across Wisconsin.

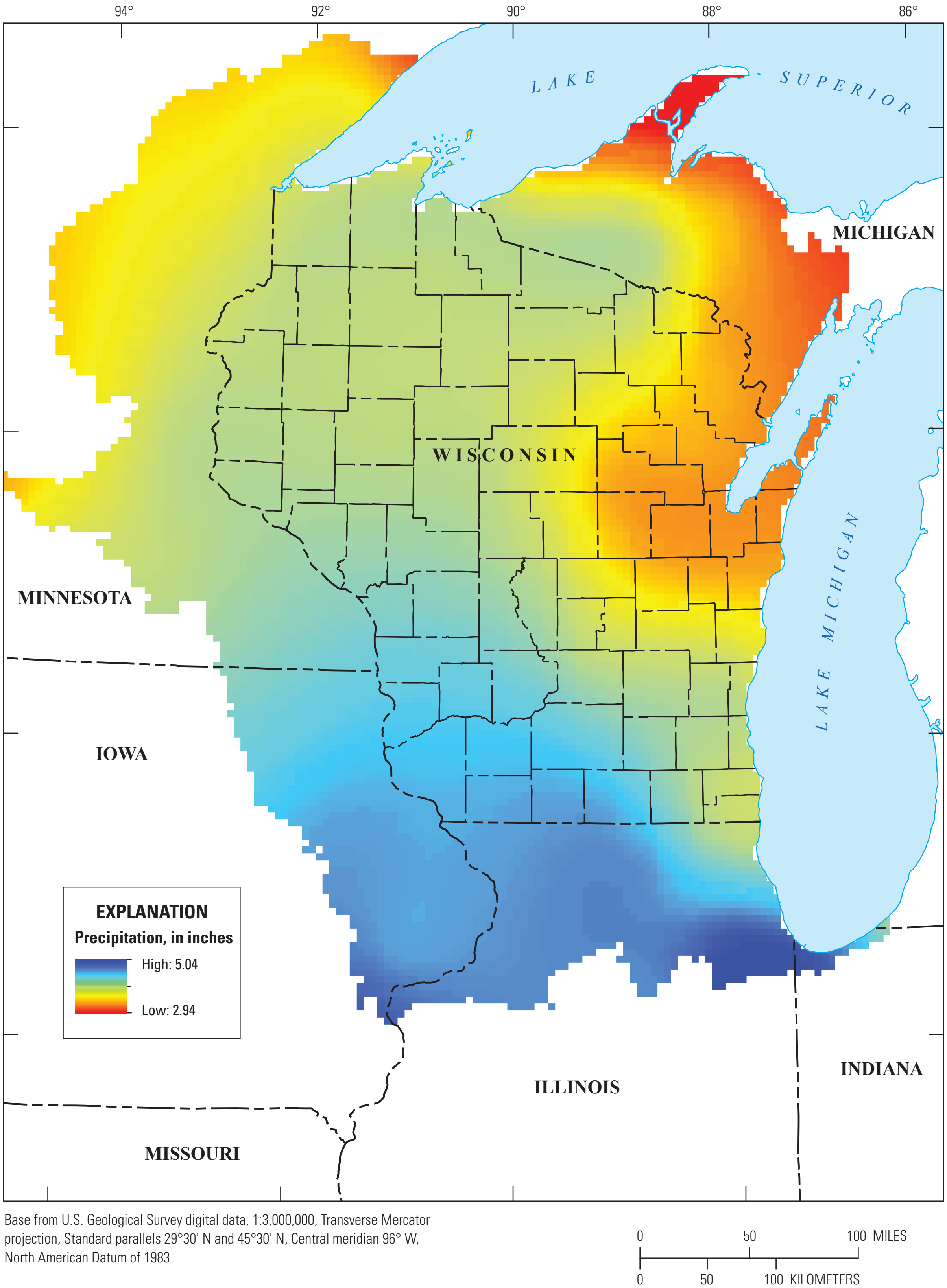

Figure 2–6. Distribution of 10-year, 24-hour precipitation across Wisconsin.

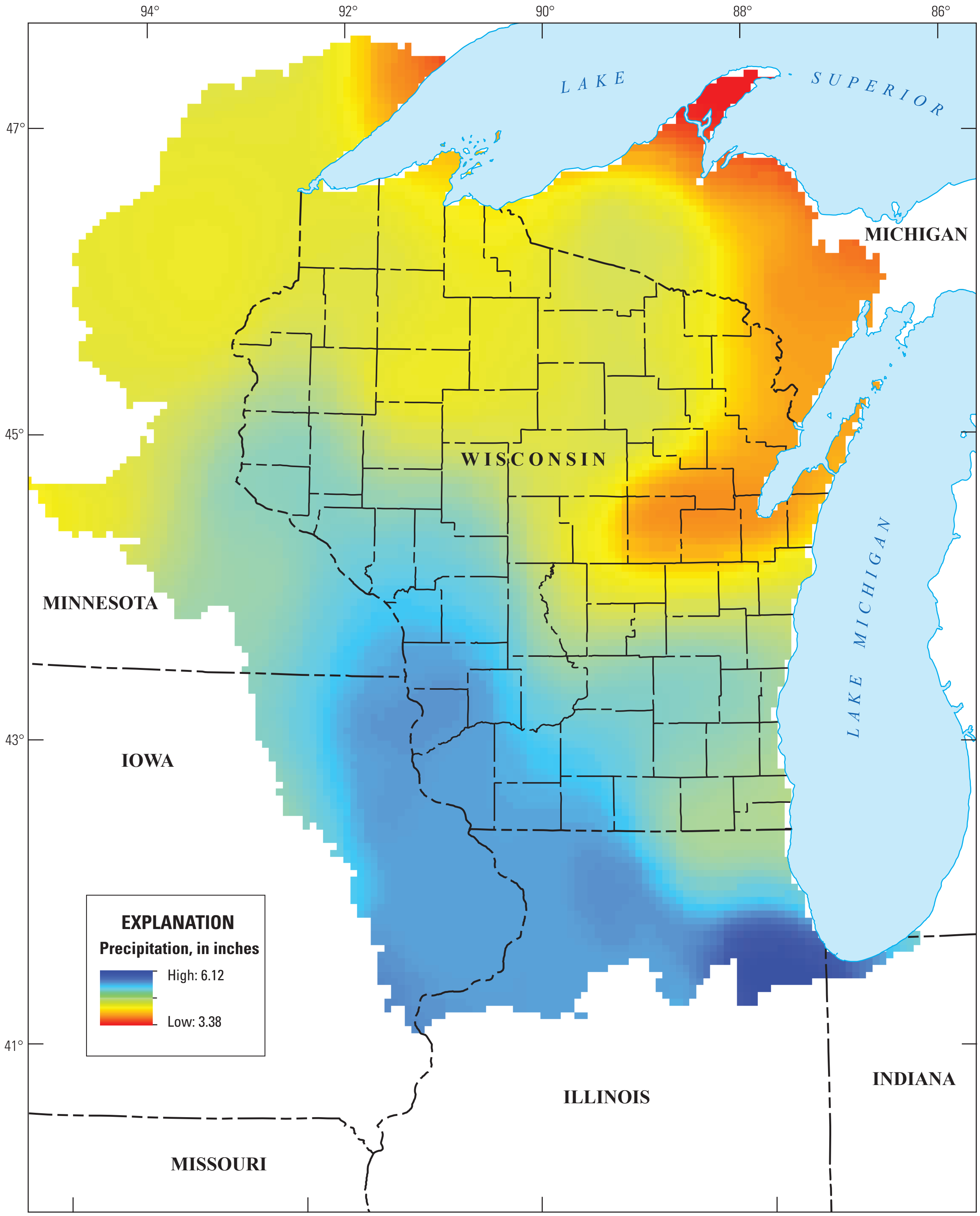

Base from U.S. Geological Survey digital data, 1:3,000,000, Transverse Mercator projection, Standard parallels 29°30' N and 45°30' N, Central meridian 96° W, North American Datum of 1983

0 50 100 MILES
0 50 100 KILOMETERS

Figure 2–7. Distribution of 25-year, 24-hour precipitation across Wisconsin.

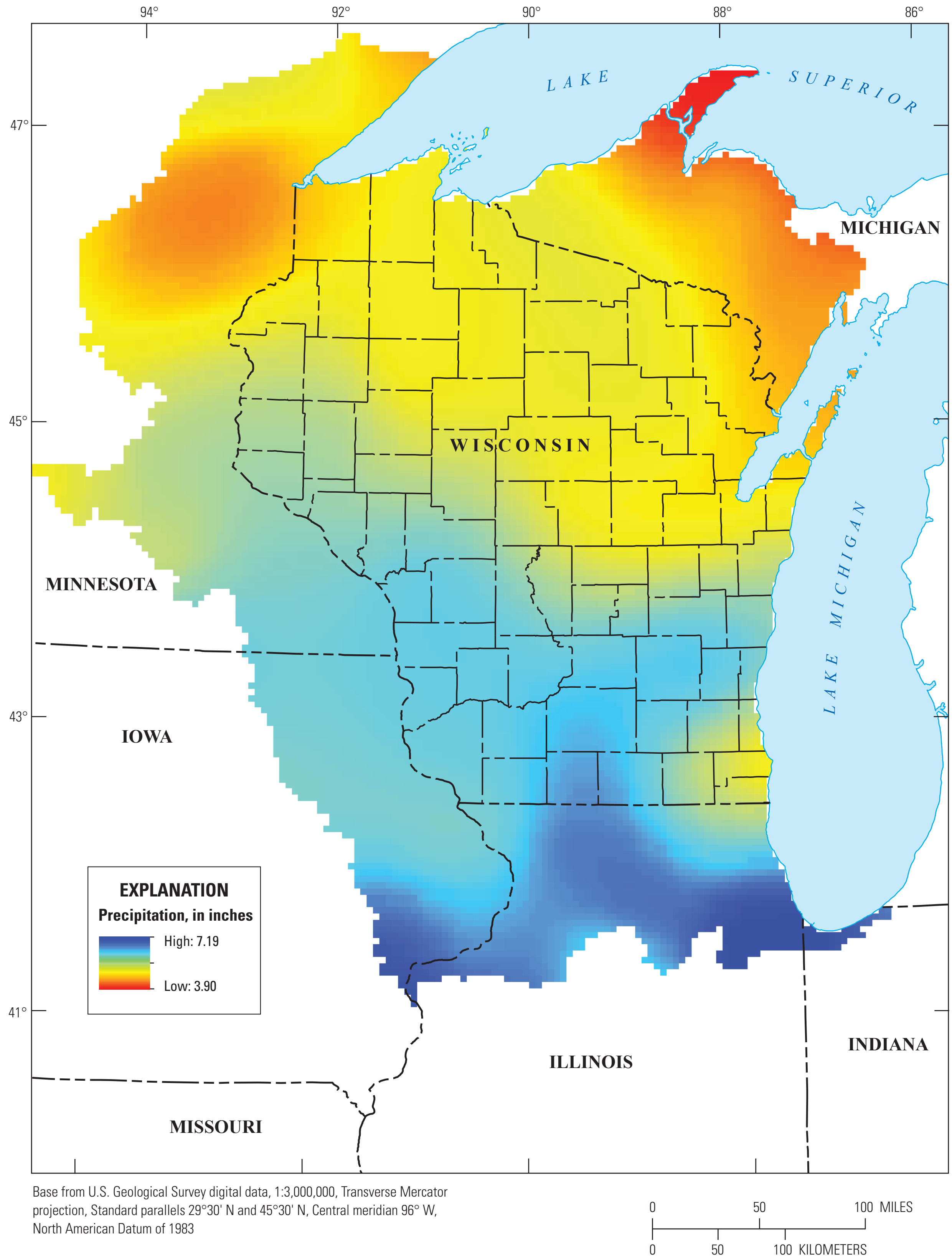

Figure 2–8. Distribution of 50-year, 24-hour precipitation across Wisconsin.

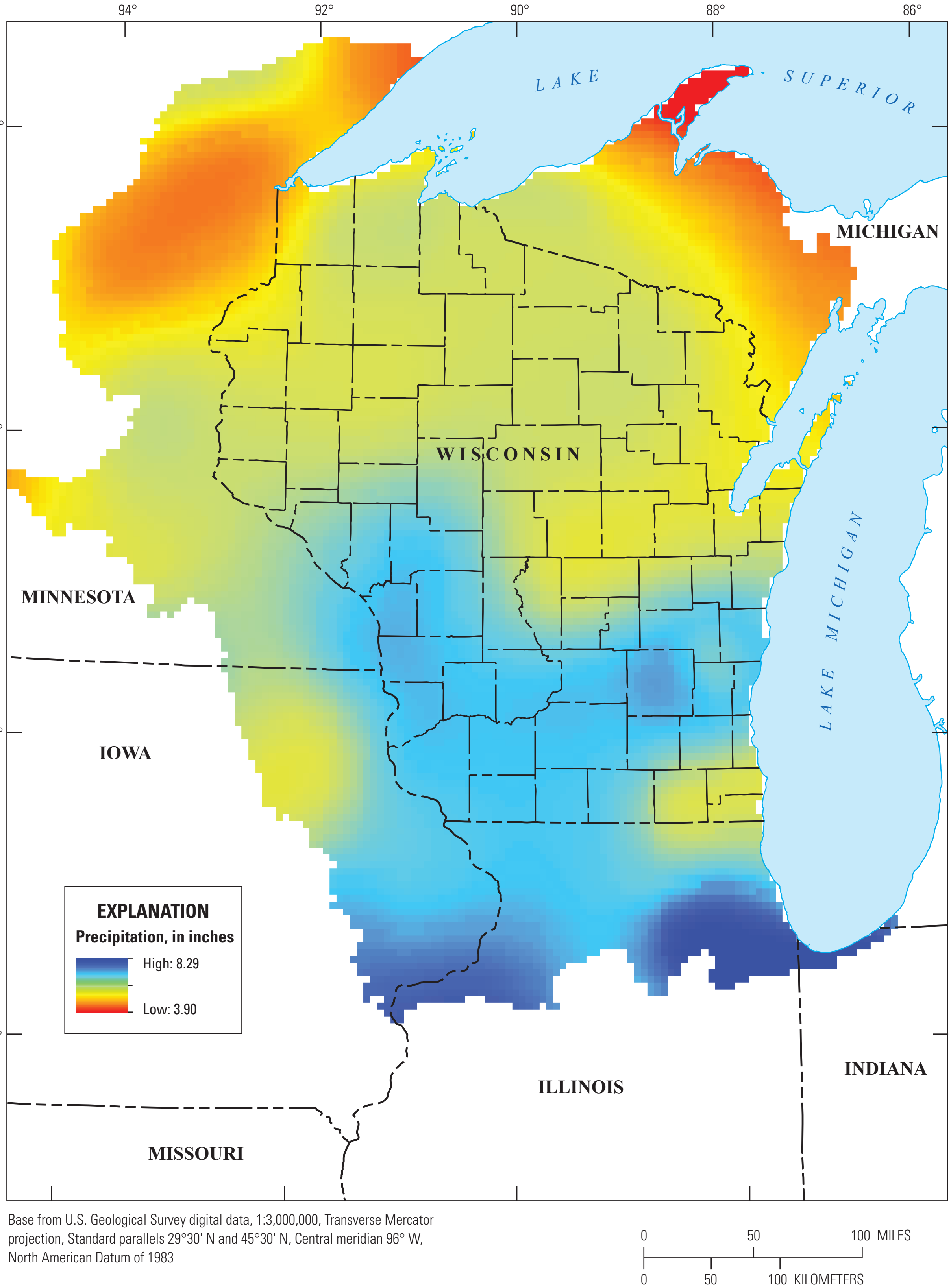

Figure 2–9. Distribution of 100-year, 24-hour precipitation across Wisconsin.

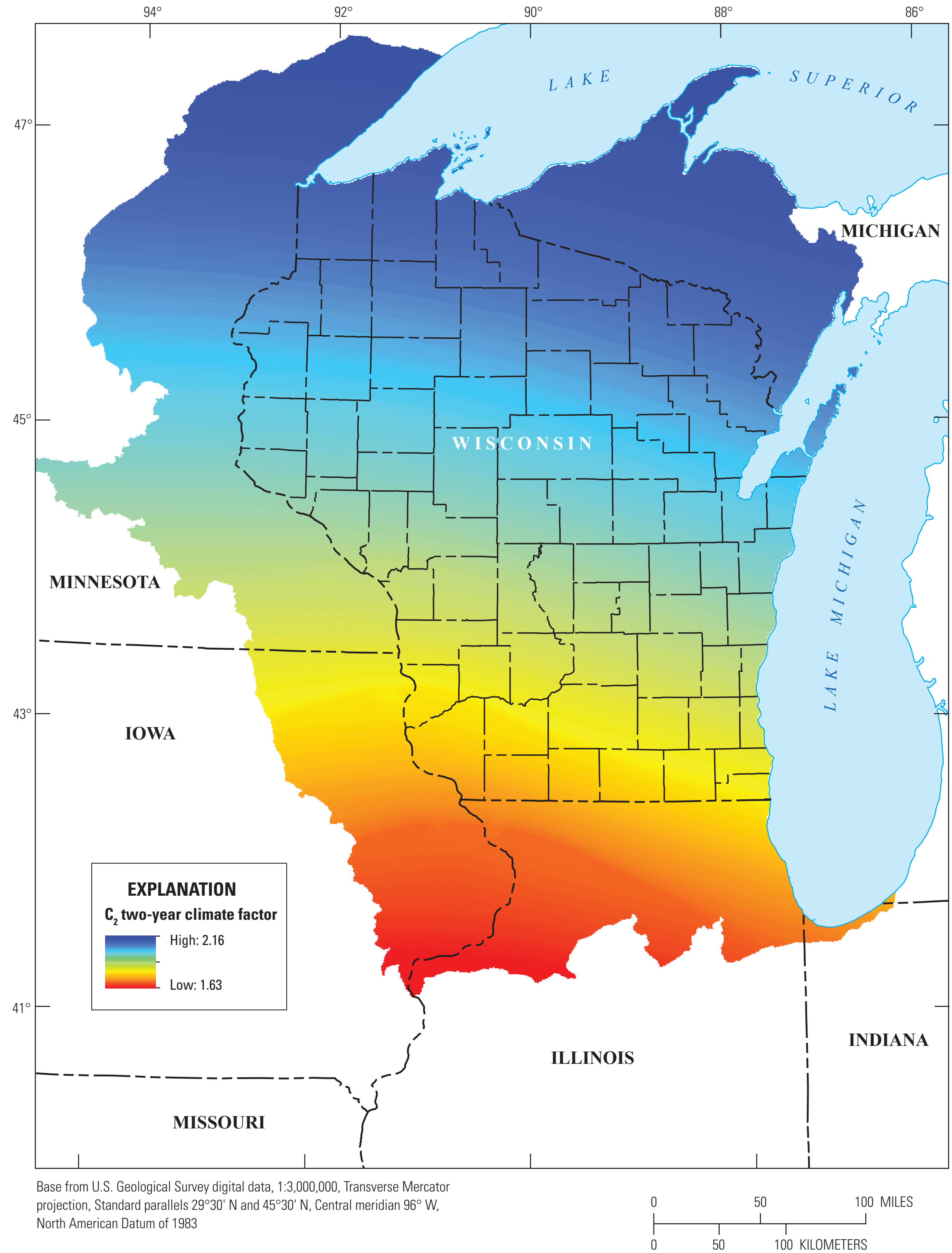

Figure 2–10. Distribution of the 2-year climate factor (C_2) across Wisconsin.

For additional information contact:
Director, Wisconsin Water Science Center
U.S. Geological Survey
8505 Research Way
Middleton, WI 53562
http://wi.water.usgs.gov

Prepared by the U.S. Geological Survey, Science Publishing Network,
Madison and Rolla Publishing Service Centers

Walker and others—**Flood-Frequency Characteristics of Wisconsin Streams**—Scientific Investigations Report 2016–5140, Version 2.2

ISSN 2328-0328 (online)
https://doi.org/10.3133/sir20165140